TALLINN UNIVERSITY OF TECHNOLOGY

School of Science

Department of Marine Systems

THE SPATIAL CONTRIBUTION OF INDIVIDUAL STATIONS TO ATDNET LIGHTNING LOCATION SYSTEM

Master's Thesis

Laura Eiber

Supervisor: Sven-Erik Enno, PhD

Co-supervisor: Prof. Sirje Keevallik

Tallinn

2017

Declaration

Hereby I declare that this master's thesis, my original investigation and achievement, submitted for the master's degree at Tallinn University of Technology has not been submitted for any academic degree. All content and ideas drawn directly or indirectly from external sources are indicated as such.

Laura Eiber

(Signature and date)

Supervisor: Sirje Keevallik

Work meets the requirements for master's thesis.

(Signature and date)

Chairperson of the defence panel:

Accepted for defence

……………………………

(Name, signature, date)

TALLINNA TEHNIKAÜLIKOOL

Loodusteaduskond

Meresüsteemide instituut

ÜKSIKUTE DETEKTORITE RUUMILINE PANUS ATDNET VÄLGUDETEKTORITE VÕRGUSTIKUS

Magistritöö

Laura Eiber

Juhendaja: Sven-Erik Enno, PhD
Kaasjuhendaja: Prof Sirje Keevallik

Tallinn

2017

TABLE OF CONTENTS

ABSTRACT

The Met Office Very Low Frequency long-range lightning location system ATDnet was examined at a station level in order to investigate the performance of its individual stations. The system consists of 10 operational sensors in and around Europe and detects lightning in Europe, Asia, Africa, South America, the Atlantic Ocean and parts of North America and the Pacific Ocean.

The average number of contributing stations and contribution ratios of individual stations per lightning event were computed for the whole spatial range of the network to check for well and poorly covered areas and problematic sensors. More than 145 million ATDnet individual lightning observations during March 2015 to August 2016 were analyzed.

The results revealed that the highest number of contributing stations occurred in large parts of the Atlantic Ocean with an average of 8−9 contributing stations out of 10. In Europe, the average number of contributing stations was 6−8. The average decreased relatively fast to the east and south of the network perimeter but much slower to the west and southwest of stations. The individual stations with the highest contribution ratio were Payerne, Eskdale and Norderney. Helsinki, Valentia and Gibraltar were the weakest contributors. Importantly, many stations were surrounded by circular modal interference bands with lower contribution ratios.

Key words: ATDnet, lightning location system, Very Low Frequency, contribution of stations

LÜHIKOKKUVÕTE

Met Office'i ülimadalsageduslikku välgudetektorite võrgustikku ATDnet'i uuriti detektorite tasandil hindamaks nende individuaalset tööd. Võrgustik koosneb kümnest detektorist, mis paikevad Euroopas ja selle lähiümbruses. ATDnet registreerib äikest Euroopas, Aasias, Lõuna-Ameerikas, Atlandi ookeanil ja vähesel määral ka Põhja-Ameerikas ning Vaiksel ookeanil.

Arvutati keskmine registreerimises osalenud detektorite arv ja panustamissuhe üksikute detektorite jaoks ühe välgusündmuse kohta kogu võrgustiku ruumilises ulatuses. Eesmärgiks oli hästi ja puudulikult kaetud alade ning problemaatiliste detektorite tuvastamine. Analüüsiti rohkem kui 145 miljonit välgusündmust, mis esinesid uurimisperioodil 2015. aasta märtsist kuni 2016. aasta augustini.

Tulemustest selgus, et kõrgeima arvuga registreerimises osalenud detektorite ala hõlmas suure osa Atlandi ookeanist. Seal registreeris ühte välgusündmust keskmiselt 8−9 detektorit. Euroopas oli keskmine registreerimises osalenud detektorite arv 6−8. Keskmine vähenes kiiremini võrgustiku perimeetrist ida ja lõuna suunas ning aeglasemalt lääne ja edela suunas. Kõige kõrgema panustamissuhtega detektorid olid Payerne, Eskdale ja Norderney. Helsingi, Valentia ja Gibraltar panustasid kõige vähem. Märkimisväärne tulemus oli ringjate modaalse interferentsi alade esinemine madalama panustamissuhtena ümber mitmete ATDnet'i detektorite.

Võtmesõnad: ATDnet, välgudetektortite võrgustik, ülimadalsagedus, detektorite panus

LIST OF ABBREVIATIONS

ATDnet – Arrival Time Difference NETwork

LLS – lightning location system

VLF – Very Low Frequency (3–30 kHz)

LF – Low Frequency (30–300 kHz)

MF – Medium Frequency (300 kHz–3 MHz)

VHF – Very High Frequency (30–300 MHz)

MDF – Magnetic Direction Finding

TOA – Time of Arrival

IMPACT – Improved Accuracy Using Combined Technology

LMA – Lightning Mapping Array

IC – intracloud lightning

CG – cloud to ground lightning

LA – location accuracy

DE – detection efficiency

INTRODUCTION

Lightning is a dangerous weather phenomenon that can cause social and economic damage. Lightning detection is important for better understanding of lightning formation, development and movement. More efficient lightning detection and thereby better prediction of thunderstorms can reduce the risk for people's lives and property.

Lightning location systems (LLSs) are nowadays the most common way to detect lightning (Nag *et al.* 2015). There is a large number of LLSs across Europe and in the world using different geolocation techniques and operating at different frequency ranges.

ATDnet (Arrival Time Difference NETwork) is a long-range LLS operated by the United Kingdom's national weather service the Met Office. ATDnet uses a variation of Time of Arrival (TOA) geolocation method called Arrival Time Difference (ATD), which detects electromagnetic waves (atmospherics or simply sferics) in the Very Low Frequency (VLF) range emitted by lightning discharges (Gaffard *et al*. 2008).

The performance of a lightning location system is traditionally assessed by measuring its detection efficiency (DE) and location accuracy (LA). ATDnet DE and LA have been assessed by comparing it against other presumably more accurate lightning location networks. There have also been some studies highlighting the negative impact of VLF propagation related waveform distortion on ATDnet DE and LA. However, there is a need for a station level assessment of the system in order to better understand how strengths and weaknesses of individual stations affect the whole network. Accordingly, the aim of the present study is to examine the contribution of individual stations over the whole spatial range of ATDnet and find the answers to the following study questions:

1. Which areas are characterized by significantly higher or lower number of contributing stations per detected lightning event?
2. Which stations are the best and the worst contributors and where are the areas with the highest and the lowest contribution ratio for each station?

3. Are there diurnal or seasonal changes in the number of contributing stations or in contribution ratios of different stations?

Results can help to assess the spatial reliability of the network as high numbers of contributing stations indicate that the full potential of the network is used and observations are as good as possible with the current sensors and network geometry. The spatial contribution ratios indicate which stations are the most important contributors in different areas and which areas would suffer in case of a failure of different stations. In addition, the results point out the best and the worst operational stations. This information can be used for network improvements.

The study is divided into five chapters. The first chapter gives an overview of the electromagnetic radiation emitted by lightning. It also briefly describes different lightning locating systems and geolocating techniques, and their quality assessment methods. The second chapter introduces ATDnet, describes previous studies about the network and defines the goals of the present study. The third chapter describes data and method, the fourth chapter presents the results and the fifth chapter discusses the findings.

1. LITERATURE REVIEW

1.1 Lightning as a source of electromagnetic radiation

A lightning flash is the result of an electrical breakdown between clouds (intracloud lightning − IC) or clouds and the ground (cloud-to-ground lightning − CG). Flashes consist many physical processes producing electromagnetic energy in radio frequency range from a few Hz to 300 MHz. In addition, lightning emits microwaves, visible light, and X- and gamma rays at higher frequencies (Rakov and Uman 2003).

The strongest radiation occurs in the VLF (3–30 kHz) band and originates from CG return strokes (e.g. Cummins *et al.* 2000). A return stroke is the most powerful part of the CG lightning flash that moves upward after a stepped leader has reached the ground. There are generally 3–5 return strokes per CG flash (Rakov and Uman 2003). Strongest emissions in Very High Frequency (VHF 30–300 MHz) range originate from electrical breakdown that is part of ionized channel formation process (e.g. Cummins *et al.* 2000). These emissions are widely detected by various ground-based LLSs.

Optical emissions are used for geolocating lightning from space. These emissions are detected after powerful return strokes which rapidly heat lightning channels. Air atoms in the channels are excited and ionized by the intense heat and emit visible light while overheated lightning channel cools down (Rakov and Uman 2003).

Optimal lightning detection method depends on user's needs. LLSs using different frequencies and geolocation methods are described in the following sections.

1.2 Lightning locating systems and geolocating techniques

LLS may be a ground- or space-based electromagnetic sensor or network of sensors, which is able to determine lightning flash location with exact time and follow intensity and movement of thunderstorms in real time (Nag *et al.* 2015).

Ground-based networks typically employ multiple sensors and a central processor. Sensors detect electromagnetic radiation produced by lightning and send the information to the central processor (Nag *et al*. 2015). The central processor finds the lightning event location by using one of the technique described in subsection 1.2.1 – 1.2.4.

Ground-based LLS sensors generally operate at frequencies from VLF to VHF. LLSs operating at VLF are called long-range systems because of the propagation characteristics of electromagnetic signals in these frequencies. Emissions in VLF propagate in the Earth–ionosphere waveguide over thousands of kilometers with relatively low attenuation (e.g. Cummins and Murphy 2009). Thus, long-range LLSs are capable of detecting lightning events as far as a few thousand kilometers from sensors (Nag *et al*. 2015). All long-range LLSs find lightning location using one of the following method: Magnetic Direction Finding (MDF − described in subsection 1.2.1), Time of Arrival (TOA − described in 1.2.2), or a combination of the two named IMPACT (Improved Accuracy Using Combined Technology − described in 1.2.3) (Cummins and Murphy 2009). VLF systems are mainly designed to respond to CG return strokes. However, the latest findings have revealed that VLF networks are also capable of detecting a considerable amount of IC flashes, which often start with powerful sferics emitted by initial breakdown processes (e.g. Enno *et al*. 2016a).

LLSs operating at Medium Frequency (MF 300 kHz–3 MHz) to VHF are short-range systems. Electromagnetic emissions in this frequency range attenuate quickly and thus VHF networks detect lightning activity only nearby the sensors (Poelman 2010). In addition to geolocating lightning event, some of the VHF systems using TOA, IMPACT or interferometry method are capable of reconstructing the path of IC and CG lightning in two or three dimensions. These networks are called Lightning Mapping Arrays (LMAs) (Cummins and Murphy 2009).

Space-based sensors locate lightning from Earth-orbiting satellites by detecting light emitted in the upward direction by IC and CG discharges. Lightning data from satellites is best for estimating global flash density (Rakov and Uman 2003). The

Optical Transient Detector (OTD), Lightning Imaging Sensor (LIS) and Geostationary Lightning Mapper (GLM) are the three most well known optical sensors, which are described in subsection 1.2.5.

The development of lightning location systems have been promoted by scientific interest and practical needs such as forecasting thunderstorms for weather services, land management entities, forest services, and public utilities. Lightning warning is also critical for aviation (Cummins and Murphy 2009).

1.2.1 Magnetic Direction Finding (MDF)

MDF systems can be divided into two general types: narrow band (tuned) direction finders and gated wideband direction finders. Both use two vertical and orthogonal loop antennas with planes (Fig. 1.1) to detect horizontal magnetic field produced by lightning. Antennas are oriented along the NS and EW direction on the ground (Rakov and Uman 2003).
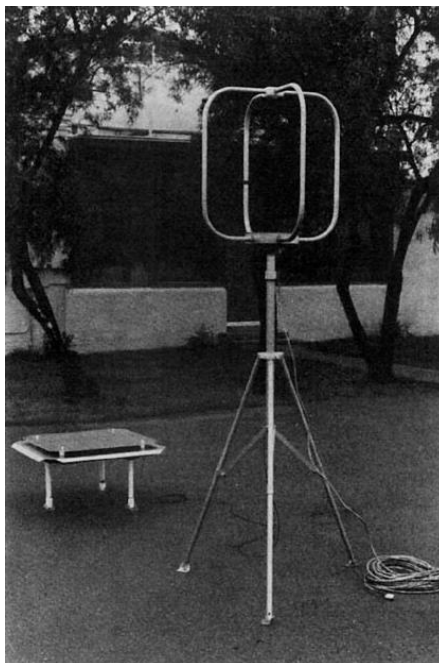

Figure 1.1. Example of a MDF sensor (Krider *et al.* 1980).

Narrow band direction finders which have been in use since 1920's and generally operate in the range of 5–10 kHz (VLF range) are less used today because of large azimuthal errors (Rakov and Uman 2003). Therefore, the following chapter describes gated wideband MDF technique developed by Krider *et al.* in 1976.

Gated wideband direction finders operate in a range of a few kilohertz to 500 kHz (VLF–MF) and respond to the initial peak of return stroke waveforms of CG flashes (Rakov and Uman 2003). By utilizing only the initial few microseconds of return stroke waveforms, gated wideband direction finders minimize azimuthal errors caused by non-vertical channel sections and reflections from the ionosphere, which are the main disadvantages of the narrowband direction finders. Errors are minimized because near the ground, where return strokes occur, most of the channels are straight and vertical and thus the magnetic field is principally horizontal (Krider *et al.* 1976).

After registering magnetic field of a return stroke, the azimuth angle of the lightning event is calculated by multiplying the lightning magnetic field and the cosine of the angle between the plane of the antenna and the discharge (Krider *et al.* 1976). To geolocate the lightning event, two or more simultaneously measured vectors are needed. The intersection point of these vectors is the lightning location. Two or more three-axis magnetic field sensors are essential to find the altitude of a lightning event (Nag *et al.* 2015).

Despite minimized polarization errors, gated wideband MDF systems have many disadvantages. For example, these systems are susceptible to site errors, which are caused by the presence of unwanted magnetic fields due to non-flat terrain and conducting objects (Rakov and Uman 2003). In addition, position errors in MDF systems are proportional to the distance between the sensors and the lightning event (Nag *et al.* 2015). Furthermore, lightning discharges detected only by two sensors are characterized by large location errors if they occur close to the line between the sensors (Cummins *et al.* 2000).

Because of problems mentioned above, MDF is not a preferred method of lightning detection nowadays. It is mainly used in combination of TOA geolocation method.

1.2.2 Time of Arrival (TOA)

TOA technique was developed in 1930's and 1940's to improve marine navigation (Colin 1970) and was first described as a method for locating lightning by Lewis *et al.* in 1960.

TOA technique bases on arrival time measurements of the return stroke peak current simultaneously at several stations on the ground (Rakov and Uman 2003). ATD (Arrival Time Difference) and TOGA (Time of Group Arrival) techniques are variations of TOA method. ATD technique measures arrival time of the whole waveform and TOGA arrival time of the wave group (Bennet *et al.* 2011). Arrival time difference between two stations defines a line of possible lightning locations. At least four stations and three lines are needed for an unambiguous lightning location. Calculating the altitude requires the presence of at least five simultaneous measurements (Nag *et al.* 2015).

TOA systems operating at VHF are LMAs, which are mainly used to study 3D development and structure of lightning discharges. Long-range systems operating at VLF and Low Frequency (LF 30–300 kHz) are used to detect the locations of CG return strokes and strong IC lightning pulses (Rakov and Uman 2003).

The main advantage of TOA systems operating at VLF is their ability to detect lightning over large areas with only a limited number of sensors. This is possible due to characteristics of VLF electromagnetic waves that bounce in the Earth-ionosphere waveguide (e.g. Cummins and Murphy 2009). Unlike MDF technique, location error of TOA systems does not depend on distance between the sensors and the lightning event (Nag *et al.* 2015; Poelman 2010).

As location accuracy is dependent on timing, insufficient time synchronization between stations causes location errors. Nowadays most of the networks use accurate

GPS timing, which minimizes the synchronization problems. Nevertheless, timing errors may be still caused by terrain elevation and soil conductivity variations, changes in the height and conductivity of the ionosphere, and registration of different parts of the waveform at different sensors (Nag *et al.* 2015).

1.2.3 Combined Technology (IMPACT)

At the beginning of 1990's a new method that combines TOA and MDF techniques called Improved Accuracy Using Combined Technology (IMPACT) was developed. IMPACT technique utilizes TOA and MDF strengths by providing range information from TOA and azimuth information from MDF (Cummins *et al.* 2000).

MDF systems need a minimum of only two sensors to geolocate a lightning event, but in that case estimated location error might be significant because of the problems mentioned in subsection 1.2.1. TOA method produces better location accuracy than MDF, but requires more sensors than two. IMPACT sensors utilize both techniques and thus only two sensors are needed to provide more accurate locations than TOA or MDF taken alone. The small number of sensors required makes IMPACT a very widely used LLS technique (Nag *et al.* 2015).

Like previously described methods, IMPACT networks can also work in different frequency ranges providing the ground contact point of a CG return stroke or mapping the full spatial extent of lightning channels. Potential problems and issues of IMPACT networks are related to disadvantages of MDF and TOA, e.g. site errors in MDF and time errors in TOA technique.

1.2.4 Interferometry

Interferometry networks operate by measuring phases of lightning pulses mainly in small bandwidth at VHF. Frequency close to 100 MHz is most effective for geolocating and mapping IC lightning (Lojou *et al.* 2009).

Interferometric VHF sensors consists of an array of closely spaced antennas with distances between individual antennas smaller than VHF wavelength (Fig 1.2). Measured phase differences between these antennas allow calculating the direction of the lightning source. At least two sensors (simultaneously measured azimuths) are needed to determine the location of an event by using triangulation (Nag *et al.* 2015). The typical baselines between sensors are 50−150 km (Cummins and Murphy 2009). Interferometric systems detection range is up to 300 km (Lojou *et al.* 2009).

Figure 1.2. Example of a VHF interferometric sensor (Lojou *et al.* 2009).

The main advantage of interferometry systems compared to other LLSs operating in VHF is the fact that interferometry does not depend on the shape of a pulse. It can easily handle noise-like bursts without a distinctive peak emitted by some cloud flashes that are difficult to use for other types of LLSs (Rakov and Uman 2003). In addition, interferometry can be used for 3D mapping of lightning channels. Compared to the TOA mapping method, interferometry requires fewer sensors and baselines between sensors are longer (typically 10–40 km for TOA). Thus, interferometry ensures larger detection range with fewer sensors (Lojou *et al.* 2009).

Despite the advantages of interferometry, TOA VHF method provides better location accuracy (thanks to a large number of closely spaced sensors) and more precise mapping for research applications (Lojou *et al.* 2009). In addition, compared to other LLSs, baselines between interferometric sensors are still very short, which makes widespread and efficient detection very expensive.

1.2.5 Optical Imaging

Optical imaging is mostly used as a space-based lightning detection technique. It has become possible with the advent of Earth-orbiting satellites. Optical sensors on satellites detect the light emitted in the upward direction by IC and GC discharges (Rakov and Uman 2003). Optical imaging technique allows calculating the time, latitude and longitude of a lightning discharge or its parts if they are sufficiently separated in space and time (Nag *et al*. 2015).

The prototype of optical sensors, named Optical Transient Detector (OTD), was launched on the Orbital Sciences Corporation Microlab-1 satellite in 1995 and stopped sending data in April 2000 (Boccippio *et al.* 2002). Follow-on of OTD, called Lightning Imaging Sensor (LIS), worked as a component of the NASA Tropical Rain Measuring Mission (TRMM) satellite's precipitation sensor suite from 1997 to 2015 (GHRC, 11.04.2017). Both were low Earth orbit instruments that detected optical pulses from lightning flashes during the day and at night (Boccippio *et al.* 2002).

The first geostationary lightning detector called Geostationary Lightning Mapper (GLM) was launched on Geostationary Operational Environmental Satellite (GOES-R) in November 2016 (Smith 2017). The geostationary sensor improves the main deficiencies of low earth orbit sensors. Low orbit satellites were able to observe a given storm only up to 90 s at once whereas geostationary sensors provide continuous hemispheric view (Finke and Hauf 2002).

The main advantage of space-based optical sensors compared to ground based systems is spatially uniform detection over large areas over many years (Finke and Hauf 2002).

The weakness of optical sensors is spatial resolution, which depends on the pixel size. For example, GLM spatial resolution is 8−14 km (Goodman *et al*. 2013), but good ground based systems can offer much more accurate lightning locations. Reducing pixel size does not enhance LA but lowers DE instead. This results from sharing the radiance of a lightning event between many pixels (Finke and Hauf 2002). In addition, optical imaging does not discriminate between CG and IC and has lower DE in daylight (Boccippio *et al*. 2002).

1.3 Assessment of geolocation accuracy

All types of LLSs have their limitations and not all flashes can be detected. Thus, LLS are widely assessed with two characteristics – DE and LA.

a) DE shows the ratio of the detected lightning events compared to the number of events that actually occurred;

b) LA is the spatial distance between detected lightning events and real lightning events (Poelman 2010).

DE and LA could be measured by validating a network against 'ground truth' or against another network. 'Ground truth' data contains locations of real flashes. These can be obtained via photo- and video observations, rocket-triggered lightning experiments and registration of strikes to instrumented towers. Such datasets are often small and contain mainly CG flashes and strokes (Nag *et al*. 2015). Thus, most of the studies use data from other LLSs as 'truth' (e.g. Bennet 2011; Poelman *et al*. 2013). In that case, the reference LLS need to be well calibrated, its performance has to be characterized independently, and the spatial ranges of the test network and the reference network need to overlap substantially (Nag *et al.* 2015). Ground-based LLS could be also validated against satellite-based optical detectors (e.g. Thompson *et al.* 2014; Enno *et al.* 2016b).

Other properties such as false alarm rate, polarity and peak current estimation accuracy, and lightning type classification accuracy are also used in order to assess the

quality of a LLS (Nag *et al.* 2015; Poelman 2010). False alarm rate is the fraction of wrongly detected non-lightning events that are included to the data (Poelman 2010).

2. ATDNET

2.1 General overview of ATDnet

ATDnet is a VLF long-range LLS operated by the Met Office (United Kingdom). The Met Office has operated VLF LLS since 1987 (Lee 1986). The current, improved LLS called ATDnet has been operational since December 2007 (Gaffard *et al*. 2008).

ATDnet uses a variation of TOA geolocation method, which registers and correlates whole waveforms to compute arrival time differences (Gaffard *et al*. 2008). One station is always selected as the reference station on the basis of good waveform quality. Time differences between the reference station and other stations determine continuous lines of all possible lightning event locations on the Earth's surface. Unambiguous lightning location is determined as an intersection point of at least three hyperbolas, thus at least four contributing stations per lightning event are needed (an example with seven hyperbolas is shown in Fig. 2.1) (Enno *et al.* 2016b). Accurate timekeeping is ensured by GPS based timing (Gaffard *et al*. 2008). During the study period, ATDnet consisted of 10 sensors (stations; Fig. 2.2) in and around Europe (Fig. 2.3), which operated at the central frequency of 13.733 kHz (Enno *et al.* 2016b).

ATDnet detects sferics which are electromagnetic waves in the VLF range. These waves propagate in the Earth–ionosphere waveguide and are emitted by CG return strokes or powerful IC pulses (e.g. Rakov and Uman 2003). ATDnet is primarily designed to detect GC lightning but recent studies have shown that ATDnet is also capable of detecting approximately 24% of IC lightning. IC flashes are mainly detected if powerful vertical initial breakdown process is involved (Enno *et al.* 2016a).

Lightning events (CG return strokes and IC pulses) detected by ATDnet are often referred to as ATDnet fixes. All fixes are checked by quality control system, which divides fixes into 'good' and 'poor'. Quality control checks fixes against predefined LA and signal quality criteria. Only good fixes are used in ATDnet data products (Enno *et al.* 2016b).

ATDnet LA and DE are highest in Europe but a lot of lightning is also detected in northern Africa, and the North Atlantic Ocean. Powerful lightning is detected as far as in central and southern Africa, South America, the South Atlantic Ocean, parts of the Pacific Ocean, the eastern seaboard of the US and in Asia (Enno *et al.* 2016b).

The accuracy and efficiency of fix locations depends mainly on the strength and quality of waveforms as arrival time differences are computed via waveform correlation. Modal interference issues can degrade waveform quality and low air conductivity may obstruct wave reaching to the sensors (described in subsection 2.2.1). In addition, network geometry affects LA, especially outside its perimeter where shallow intersection angles of fix location hyperbolas lead to larger location errors. The fewer stations contributing, the less reliable are the results (Enno *et al.* 2016b).
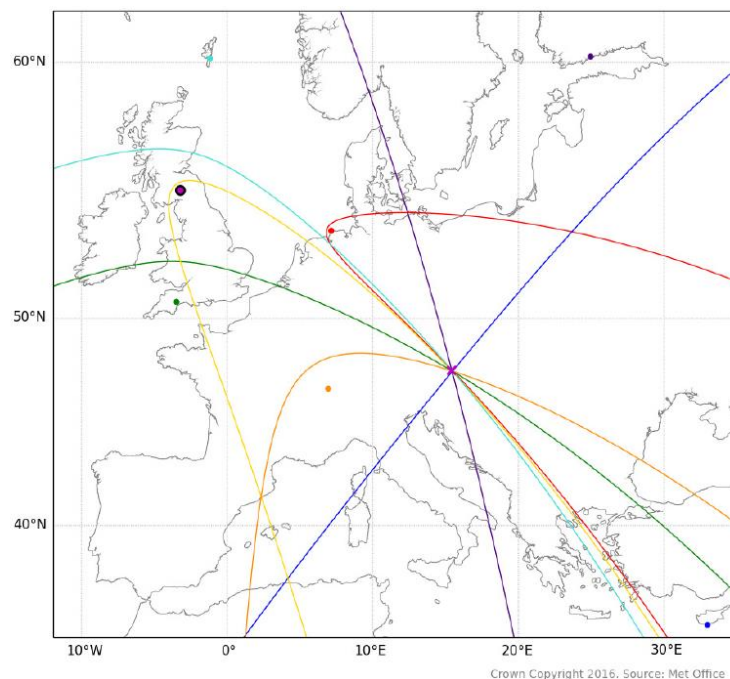

Figure 2.1. Example of an ATDnet fix location with eight contributing stations. Intersection of seven hyperbolas give the location of the event (purple cross). The reference station is marked as purple dot with a bold edge (Enno *et al.* 2016b).

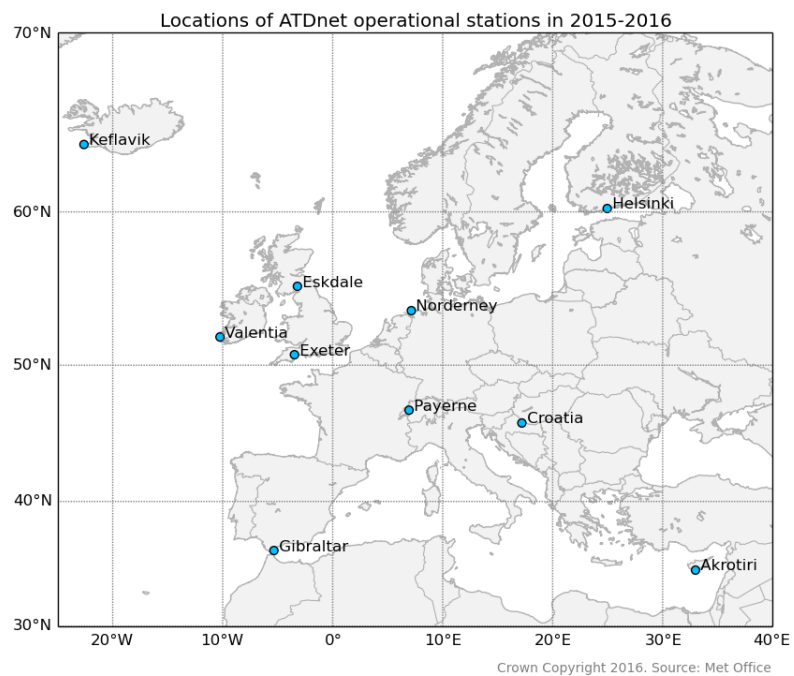Figure 2.2 ATDnet sensor located in Norderney (Bennet *et al*. 2011).

Figure 2.3. Locations of ATDnet operational stations in 2015–2016.

2.2 Previous studies about ATDnet

2.2.1 VLF propagation and modal interference effect on ATDnet

As ATDnet location accuracy depends on waveform shape, it is important to study VLF propagation and modal interference. Modal interference is noticed to be serious problem for ATDnet as it distorts waveform shape.

Propagation in the VLF can occur along the surface or via reflections between the ground and the ionosphere. Waves with different propagation paths are accordingly called 'groundwaves' and 'skywaves'. Propagation between a lightning event and a sensor closer than 1000 km is mainly related to groundwaves whereas propagation beyond 1000 km is dominated by skywaves (Volland 1995).

As different parts of sferics reach the ionosphere in different places, the number of bounces between the ground and the ionosphere may vary. The number of reflections from the ionosphere defines the number of the propagation mode. Higher order modes travel relatively larger distances, thus their apparent velocity is slower compared to lower order modes. Moreover, phases of different skywave modes are shifted relative to each other resulting in interaction between different modes. This results in waveform shape changes including significant distortion if interacting modes are in anti-phase. Waveform shape changes due to interactions of different propagation modes are called modal interference. Modal interference can be caused by both, skywave-skywave and skywave-groundwave interactions (Budden 1957).

The intensity and spatial pattern of modal interference changes with diurnal changes in the height of the ionosphere. Ionospheric height is higher at night, reaching to approximately 88.5 km, and lower during the day reflecting VLF waves at a height of approximately 70 km. Diurnal variability of ionospheric height is due to absence of solar radiation at night (Kikuchi 1986)

There are four studies (Gaffard *et al*. 2008; Bennet *et al*. 2010b; Bennet *et al.* 2011; Hudson 2014) about the effect of modal interference on ATDnet. All of them observed

pronounced waveform distortion within certain distance ranges from lightning and attributed it to modal interference.

Authors found clear differences in the spatial pattern of modal interference between night and day using signal-to-noise ratio measured by ATDnet stations. Signal-to-noise ratio is a measure of how much the waveform stands out above noise. Low signal-to-noise ratio leads to weaker and less reliable waveform correlation. Gaffard *et al*. (2008) and Bennet *et al.* (2011) noticed significant waveform correlation degradation in a region centered ~450 km from stations during the daytime whereas at night the deepest degradation occurred at distances of ~600 km and ~2100 km from stations. In addition, narrow reduction occurred ~300 km and a broader but smaller reduction ~3600 km from stations (Gaffard *et al*. 2008; Bennet *et al.* 2011). Modeled ionospheric heights for these distances were in close agreement with the observed interference patterns (Bennet *et al*. 2010b; Bennet *et al.* 2011).

A VLF waveform propagation model for ATDnet (Hudson 2014) agreed with the daytime interference zone and two closest nighttime interference zones 300 km and 600 km from stations. At the same time, any minima at distances greater than 1000 km were difficult to distinguish for the model. In addition, the model showed that the impact of modal interference on ATDnet is strongest at night when interference zones of multiple stations overlap in Western Europe (Hudson 2014).

VLF propagation could be also affected by terrain and ground conductivity. Propagation losses are smaller over areas with high conductivity that make sferics easier to detect (Wait and Spies 1965). For example, ATDnet has shown better DE over the oceans due to higher air conductivity over salty water (Enno *et al*. 2016b).

2.2.2 Studies about ATDnet detection efficiency and location accuracy

Most studies about ATDnet DE and LA compare the network against other lightning detection networks. Gaffard *et al.* (2008) compared ATDnet with French and Austrian LLSs during a one-week time period. It was found that ATDnet detected on average

6% more strokes than Meteo-France, but at the same time, Austrian LLS called ALDIS registered two times more strokes than ATDnet. Big differences between ATDnet and ALDIS could result from ALDIS recording lower peak current lightning than ATDnet.

ATDnet was compared to four different networks in different regions during a 10-day period by Bennet *et al*. (2010a) study. The median location error of ATDnet was 2.9 km compared to Météorage in France, 4.9 km compared to NORDLIS in Finland, 21 km compared to BrasilDAT in Brazil and 5.0 km compared to ALDIS in Austria. ATDnet had comparable CG lightning DE of ~50–90% over Western Europe and Finland in the daytime.

Bennet (2011) compared ATDnet with WWLLN (The World Wide Lightning Location Network) in the tropical North Atlantic in January and June 2010. The study revealed that ATDnet detects approximately three times more strokes than WWLLN.

Poelman *et al*. (2013) compared spatial and temporal lightning observations of three LLSs to estimate their DE and LA. The systems included long-range ATDnet, a regional SAFIR network operated by the Royal Meteorological Institute of Belgium (RMIB) and a sub-continental French lightning location network operated by Météorage (MTRG). The study period was May to September in 2011 and 2012. Results showed that ATDnet detected 69−80% of MTRG and 60% of SAFIR flashes in Belgian region. The median location error was accordingly 2.8–3.0 and 7.5 km. The noteworthy finding was that ATDnet also detected 25% of MTRG cloud flashes.

Enno *et al.* (2016a) validated ATDnet against a LMA called HyLMA to investigate ATDnet flash detection efficiency with the main focus on IC detection. Three storms (in September 2012) in the south of France were selected for the study. The overall ATDnet DE was found to be approximately 89% for CGs and 24% for ICs. Most of IC detections were related to initial breakdown process and vertically extensive ICs were detected with higher efficiency.

The latest study about ATDnet DE (Enno *et al.* 2016b) compared ATDnet with a satellite based optical sensor LIS. The study period was 2008–2014 and the study area

was confined to LIS data domain (38°N–38°S; 180°W–180°E). Results revealed that ATDnet performs best over the North Atlantic Ocean and the Mediterranean basin, where it detected approximately 20–30% of LIS flashes. In the Caribbean Sea, northern Africa and the northeastern part of South America ATDnet DE was around 10%, and in other regions it remained below 10%. The results of this study are considered encouraging because study area was out of the ATDnet perimeter and ATDnet was originally designed to detect CG flashes whereas LIS detects all types of lightning and is possibly more sensitive to ICs.

2.3. The main goals of the present study

As demonstrated above, many studies have compared ATDnet against other networks to estimate its DE and LA. In addition, there are some studies about the impact of VLF propagation and modal interference on waveform quality. The present study is the first one that examines the system at a station level where the following questions need to be answered:

1. Are there areas with significantly higher or lower number of contributing stations? In which areas ATDnet has a high number of contributing stations and thus the full potential of the network is used?

2. Are the spatial variations in the number of contributing stations attributable to the configuration of the network or to environmental factors such as surface conductivity and zones of modal interference?

3. Which stations are the best and the worst contributors? Which are the areas of the highest and lowest contribution for each station? Which areas would suffer in case of failure of different stations?

4. Are there areas with seasonal changes in the number of contributing stations or in contribution ratios of individual stations?

5. Are there diurnal changes in the number of contributing stations or in contribution ratios of individual stations? Are these changes directly

attributable to diurnal changes in the height of the ionosphere and its impact on VLF propagation?

The objective of the present study is to find answers to the questions above. Results can help to assess the reliability of ATDnet lightning locations and draw attention to sensors that need improvement. Thereby the results of the study contribute to ATDnet future developments towards higher detection efficiency and improved location accuracy.

3. DATA AND METHOD

3.1 ATDnet data

For the current study, preprocessed output from ATDnet database was provided. The data contained daily binary array files (.npy) with year, month, day, hour, minute, second, latitude, longitude, arrival time differences and quality (good or poor) of every detected fix. In addition, the Met Office provided a set of Python modules with different functions that were previously used in ATDnet research and development. Some of those functions were used in the present study.

The study period was 18 months − from March 2015 to August 2016 and contained more than 145 million fixes with good quality. The period was chosen because of the stability of the network configuration. Throughout the 18 months, there were no changes in the number and locations of ATDnet sensors and the system was free of major sensor outages. As a result, in seasonal analysis six months worth of data was available for spring (March to May) and summer (June to August) whereas only three months was available for autumn (September to November) and winter (December to February).

The study area was global and extended from 80°N to 80°S. Only areas around the poles were not included due to virtually non-existing lightning activity. Used grid cell size was 1°x1°.

3.2 Method

Data was processed using the Linux operating system and Python programming language (version 2.7). Two main Python scripts were written.

The first script created four-dimensional (4D) monthly numpy arrays from initial binary files. Output of the script contained computed data, day, latitude and longitude. The computed data included two values:

a) The total number of fixes per grid cell and the total number of contributing stations per grid cell; or

b) The total number of fixes per grid cell and the total number of fixes detected by a given station per grid cell.

Data type a) was necessary for spatial distribution of the average number of contributing stations and data type b) for spatial distribution of the contribution ratio of a given station.

The schema of the script that was used for computing monthly 4D numpy arrays of the total number of fixes per grid cell and the total number of contributing stations per grid cell is presented in Appendix 1.

The script started with importing necessary modules and functions, including three functions provided by the Met Office. After importing modules and setting the initial values (year, month, and days in the month), the first provided function named *initialisegrids* created a global (360°x160°; or European 110°x65°) latitude and longitude grid. Next, empty arrays for the numbers of contributing stations and total fixes were created. The main part of the script started with a *for* cycle, which worked through all days in the selected month and filtered out good fixes (and daytime or nighttime fixes if necessary). After that, another *for* cycle extracted latitudes, longitudes and numbers of contributing stations for all good fixes. Subsequently, two other functions from the provided modules were used. First of them, a function called *bintotals,* calculated the total number of fixes per grid cell using latitudes and longitudes of fixes extracted by the previous *for* cycle. Secondly, a function called *binsums* computed the totals of the numbers of contributing stations per grid cell. These results were saved into daily 2D spatial arrays which in turn were saved into a monthly 4D array. After working through all days of the month, the 4D array was saved as a numpy binary array file.

The script described above was slightly modified to get a monthly 4D array containing total number of fixes and total number of fixes detected by a given station per grid cell.

Most importantly, an additional *for* cycle iterating through all stations was created and spatial grids were computed separately for every station. After filtering out good fixes, the *for* cycle separated fixes detected by a given station and extracted their latitudes and longitudes. Next, functions *bintotals* and *binsums* were used. In this case, *binsums* calculated the total number of fixes detected by a given station. An output file containing the monthly 4D array was created for every station. Overall schema of this script is presented in Appendix 2.

Time ranges of 10:00−17:00 UTC and 21:00−04:00 UTC were used for filtering out daytime and nighttime fixes, respectively.

The second main script read in the monthly 4D numpy arrays prepared by the first script and plotted maps of a) average number of contributing stations per grid cell and b) contribution ratio of a given station per grid cell.

After importing modules and setting the initial values, three main functions were written and used to get the result. The first function, called *retrievegrids*, retrieved daily grids from numpy binary array files and summed them up over a given month or season. In order to sum the input arrays, the function created empty 2D arrays (360°x160° for global maps, 110°x65° for European maps) and used a *for* cycle, which read in one month worth of daily data and summed it up into the empty arrays. In addition, monthly average contribution ratio was computed for each station and saved into a CSV file. The data was latter plotted in MS Excel.

The second function, called *calcdensity,* used the summed up monthly grids and calculated the average number of contributed stations or contribution ratio of a given station per grid cell. Arrays containing the total numbers of contributing stations or numbers of fixes detected by a given station were divided by an array containing the total number of fixes per grid cell. The result was saved into a new array. Note that grid cells with less than 10 ATDnet fixes during the study period were omitted in order to avoid spurious results due to very small samples.

The third function, called *plotdensity* used the output of the second function and plotted it on a raster map. This function used many mapping functions provided by the Met Office, which were adjusted to meet the requirements of the current study.

These three functions were used in the same order as they are described above. The overall schema of the second main script is represented in Appendix 3.

4. RESULTS

4.1 Number of contributing stations per fix

The spatial distribution of the average number of contributing stations is represented in this section. The average number of contributing stations is always ≥ 4 as ATDnet requires at least 4 contributing stations for an unambiguous lightning location. Grid cells with less than 10 fixes are shown in gray as the amount of data was too small for reliable statistics.
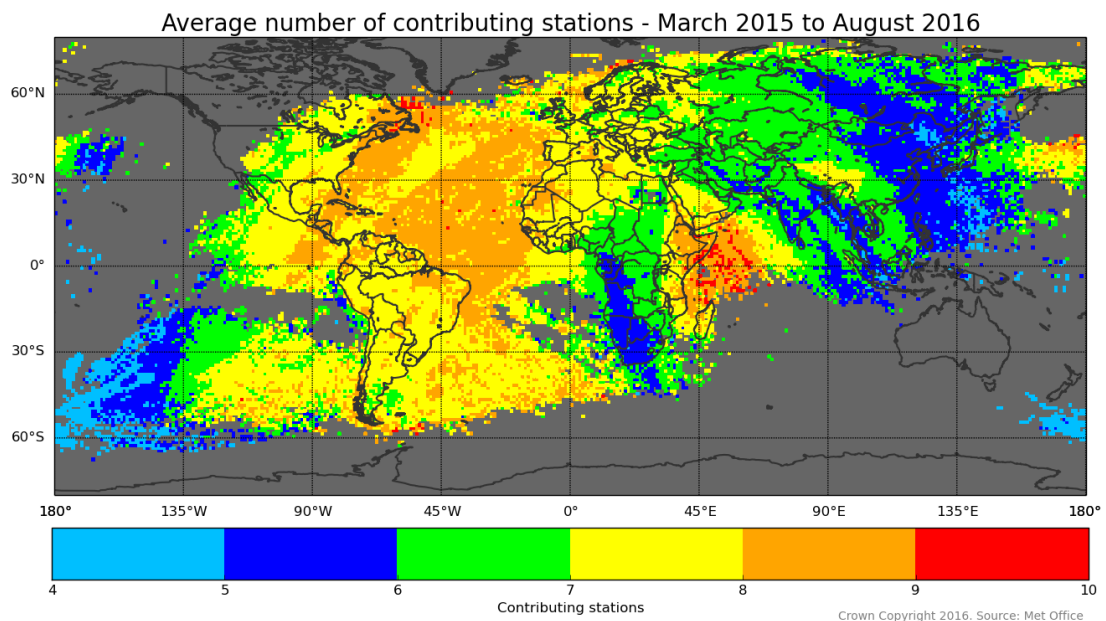

Figure 4.1. The average number of contributing stations from March 2015 to August 2016.

The spatial distribution of the average number of contributing stations during the study period is presented in Fig. 4.1. The area with the highest number of contributing stations encompassed northwestern part of the Indian Ocean where the values reached 9−10. In addition, large areas with 8−9 contributing stations occurred in the Atlantic Ocean. More than 7 stations contributed in Southern Europe, the Mediterranean, the northwestern part of Africa, South-America and the eastern part of North America. In Europe, the average number of contributing stations was 6−8, decreasing eastward.

Higher number of contributing stations in these areas suggests that the full potential of the network is used and obtained lightning locations are as good as other limiting factors such as network geometry allow.

An average of 6−7 contributing stations per fix was observed in Central Asia and Central Africa region. In the southeastern part of the Pacific Ocean, southern part of Africa, areas in India and Indonesia, and eastern part of China and Russia 5−6 stations contributed. The number of contributing stations dropped below 5 in large areas in South Pacific Ocean and little smaller areas in Eastern Asia and Pacific nearby.

Differences between night and day can be seen in Fig. 4.2 and Fig. 4.3. The average number of contributing stations was higher by approximately one station at night. The most evident diurnal change occurred in large areas in Atlantic Ocean. During the daytime, on average 7−9 stations contributed there, whereas at night the number of contributing stations per fix was 8−10. In addition, instead of 7−8 contributing stations during the day, 8−9 stations contributed in Southern Europe, the Mediterranean Sea, the northern part of Africa and South America at night. The average value of contributing stations in the whole Europe increased from 6−8 during the day to 7−9 at night. Furthermore, at night, the region with 7−8 stations in Asia extended further eastward and reduced the size of the area with 5−6 contributing stations. The only region with decreased value of contributing stations at night occurred in Southern Africa.
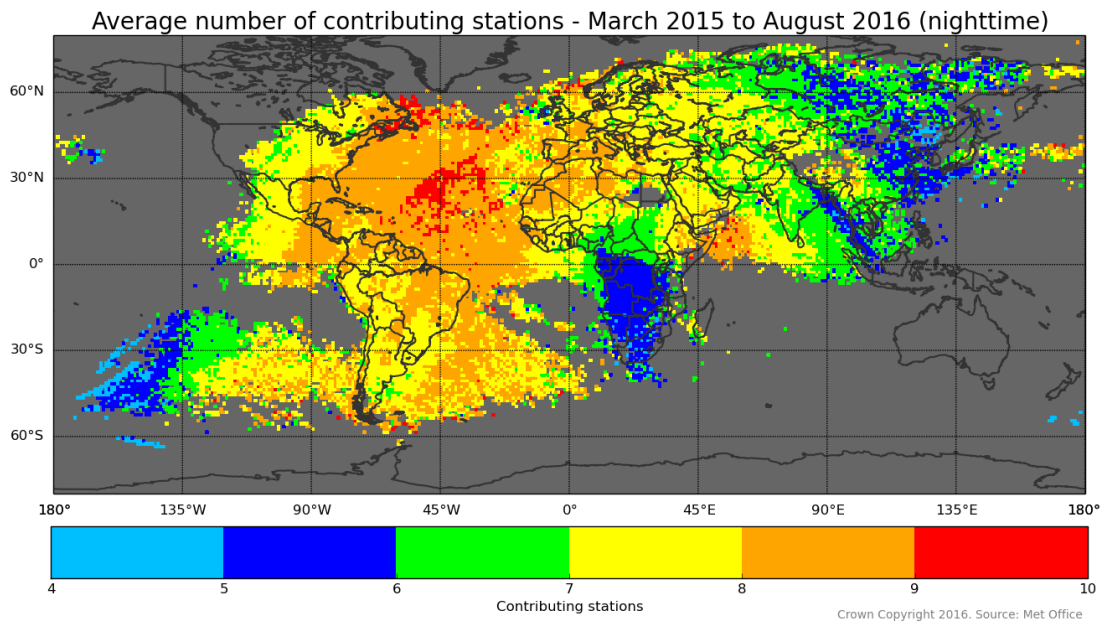
Average number of contributing stations - March 2015 to August 2016 (nighttime)

Figure 4.2. The average number of contributing stations from March 2015 to August 2016 at night.

Average number of contributing stations - March 2015 to August 2016 (daytime)
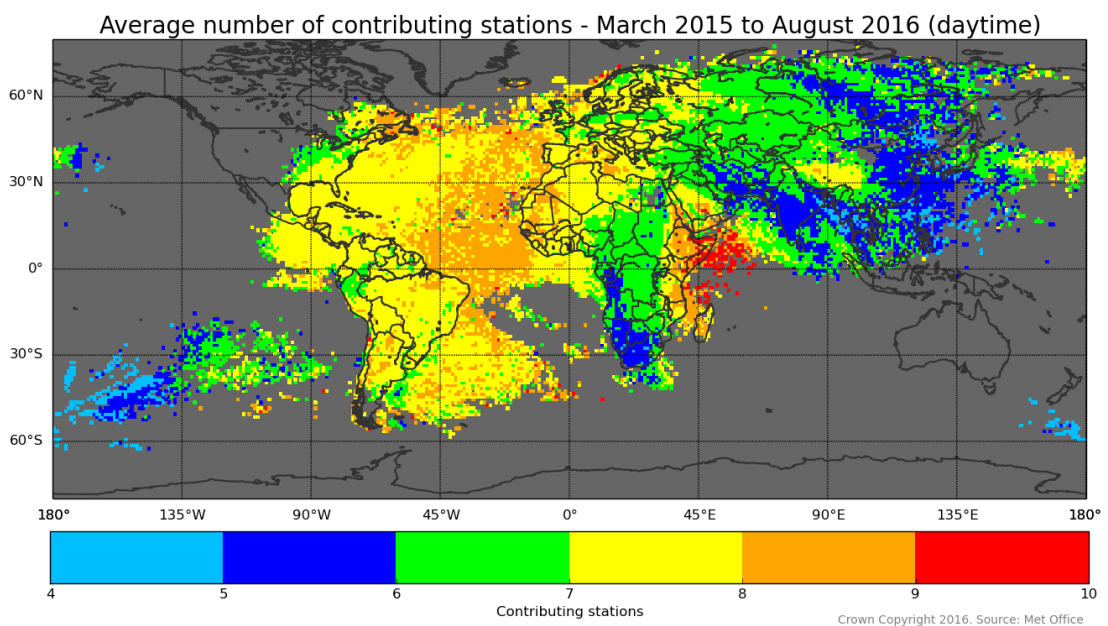
Figure 4.3. The average number of contributing stations from March 2015 to August 2016 during the daytime.

Seasonal differences in the number of contributing stations were small. They were most noticeable in relatively small areas in the middle of the Atlantic Ocean, where the number of contributing stations dropped from 8−9 to 5−6 in spring and winter. The Atlantic Ocean as a whole had slightly higher number of contributing stations in winter and autumn. In addition, increased number of contributing stations is visible in winter in and around Europe (Fig. 4.4).
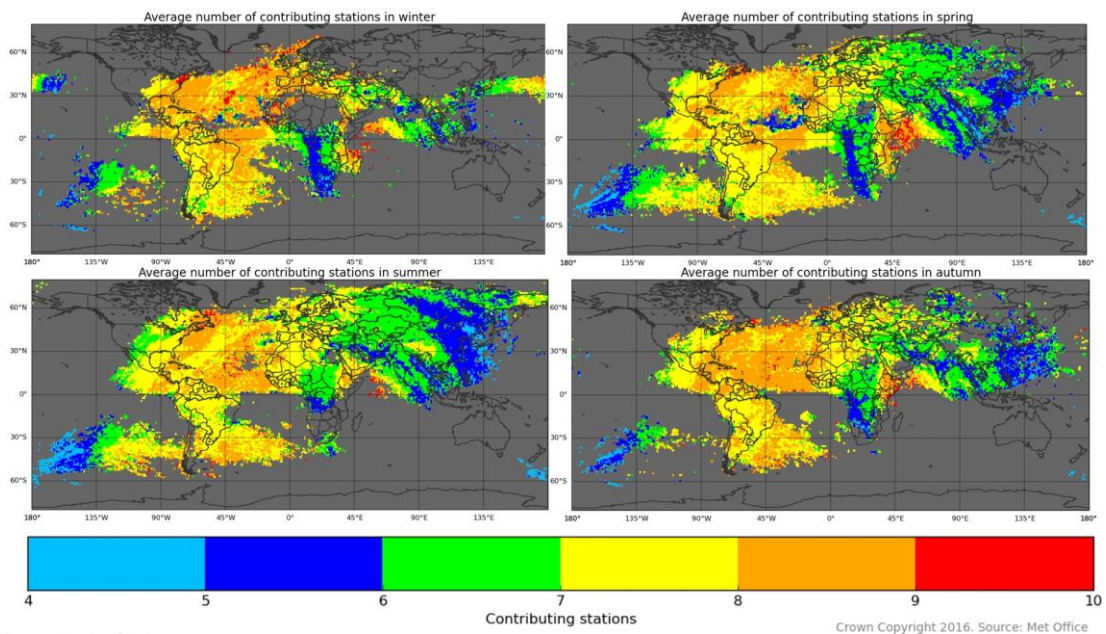

Figure 4.4. The average number of contributing stations in winter (upper left), in spring (upper right), in summer (bottom left) and in autumn (bottom right) from March 2015 to August 2016.

4.2 The average contribution ratio by stations

The average contribution ratio of each station is represented in subsections 4.2.1−4.2.10. The location of the stations is marked with the white star. The subsections are ordered starting with the station with the highest overall contribution ratio. Spatial differences in contribution ratios between day and night are also assessed with corresponding maps in Appendixes 4−13. Contribution ratios showed no

remarkable seasonal variations, therefore there are no seasonal differences described in the section.

In addition, circular bands with dropped contribution ratios were observed within approximately 2000 km from most stations. During the daytime generally one and at nighttime two circles with lower contribution ratio occurred. These circles correspond to modal interference zones. As the impact of modal interference on ATDnet lightning detection is significant, maps of interference zones are presented for every station.

Contribution ratios of individual stations by regions are described subsection 4.2.11 and monthly contributing ratios are presented in subsection 4.2.12.

4.2.1 Payerne station

Payerne was characterized by the best contribution ratio. It detected on average 96% of all ATDnet fixes. Spatially, most of the areas had very high contribution ratio, extending to 90−100%. Contribution ratio decreased in northwest-southeast direction from Central Asia to South Asia where Payerne generally contributed to 50−90% of fixes, with some spots dropping below 50%. The worst contribution ratio of Payerne occurred in the northeast of Russia (0−50%) (Fig. 4.5).

Global differences between day and night were very small. The main difference occurred in Central Asia and India, where the contribution ratio increased approximately 10−30% at night compared to the daytime (Appendix 4).

Despite of the small global differences between day and night, clear interference zones were observed in nighttime Europe, where the contributing ratio was 10−40% lower. In addition, lower contribution ratio also occurred in a half-circle shaped band closer to the station in the daytime (Fig. 4.6).
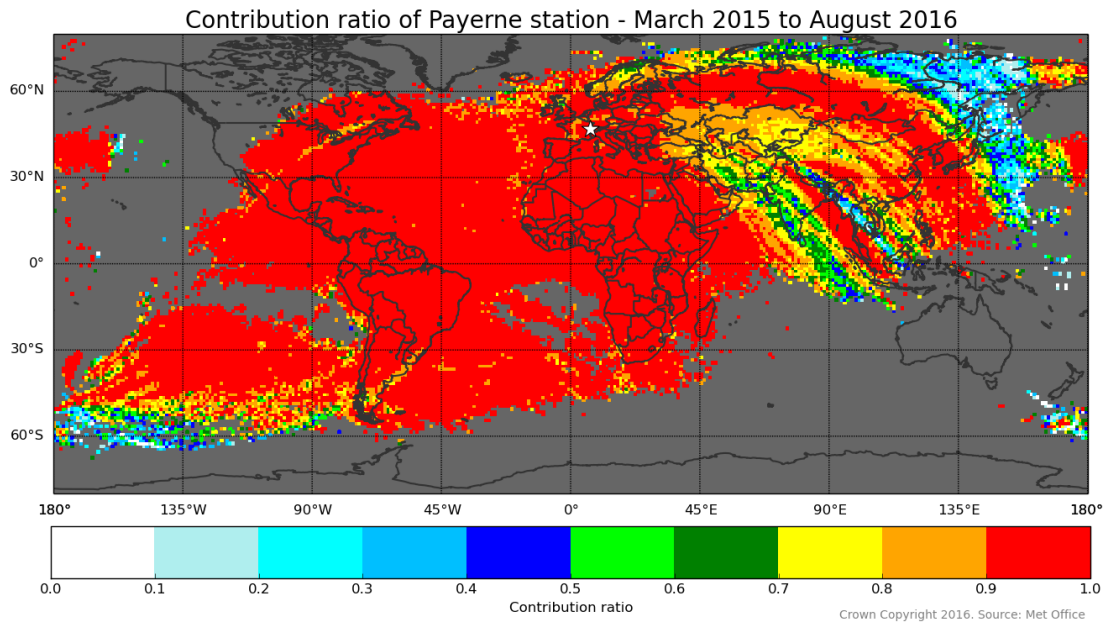
Contribution ratio of Payerne station - March 2015 to August 2016

Figure 4.5. The average contribution ratio of Payerne station from March 2015 to August 2016.

Contribution ratio of Payerne station in Europe - March 2015 to August 2016
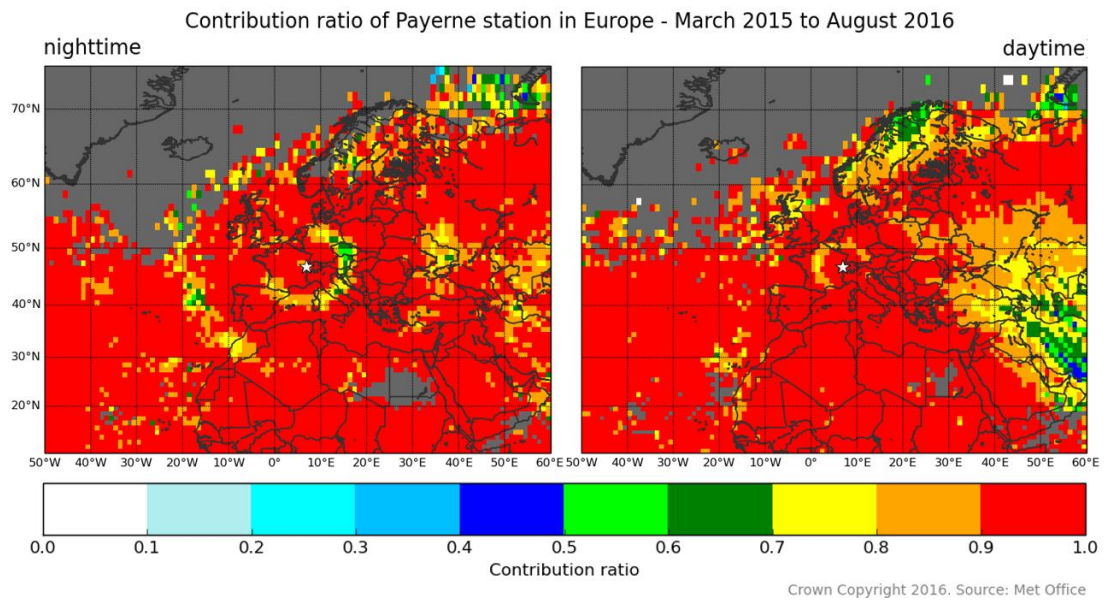

Figure 4.6. The average contribution ratio of Payerne station in Europe from March 2015 to August 2016 at night (left) and during the day (right).

4.2.2 Eskdale station

Similarly to Payerne, Eskdale contributed to 90−100% of fixes in most areas. A little lower contribution ratio (70−90%) occurred within a north to south directed swath through Africa. The lowest contribution ratio, 0−50%, occurred in a northwest-southeast directed area through East Asia (Fig. 4.7). The global average contribution ratio of Eskdale station was 92%.

The most obvious difference between daytime and nighttime contribution ratios occurred in Southern Africa, where the ratio was much higher in the daytime. During the day, the station contributed to 90−100% and at night only to 40−70% of all registered fixes (Appendix 5).

Eskdale station also showed clear interference zones with lower contribution ratio at night in Europe. Compared to Payerne, the boundaries of the zones are more diffuse and an additional zone could be noticed as semicircular band from East-Turkey to the Canary Islands. In the daytime, lower contribution near the station is visible but there is no clear circular band (Fig. 4.8).
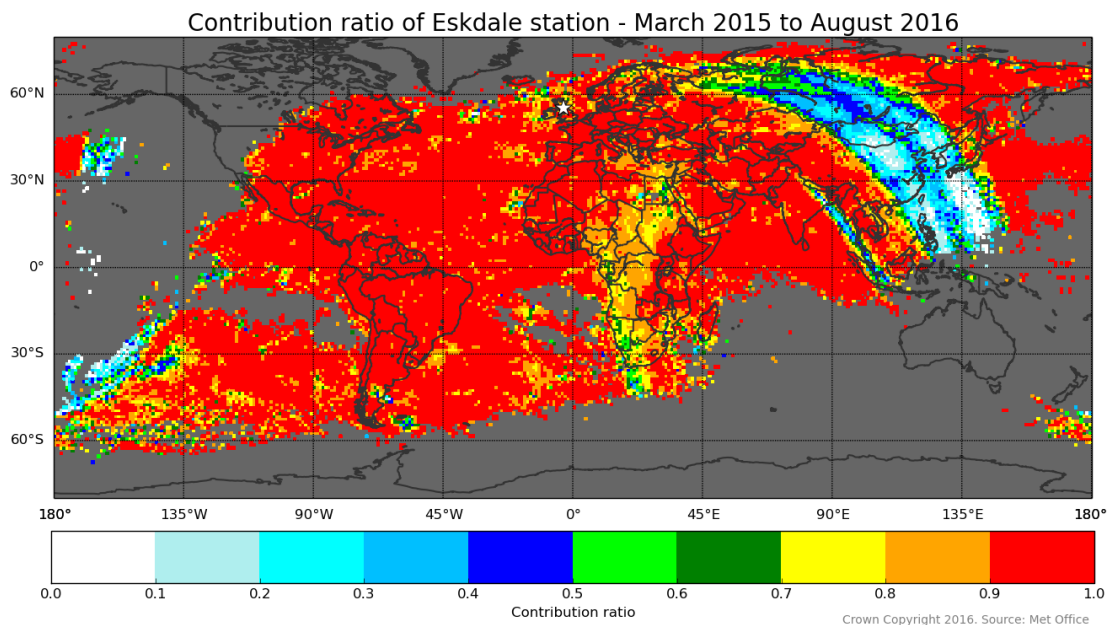

Figure 4.7. The average contribution ratio of Eskdale station from March 2015 to August 2016.
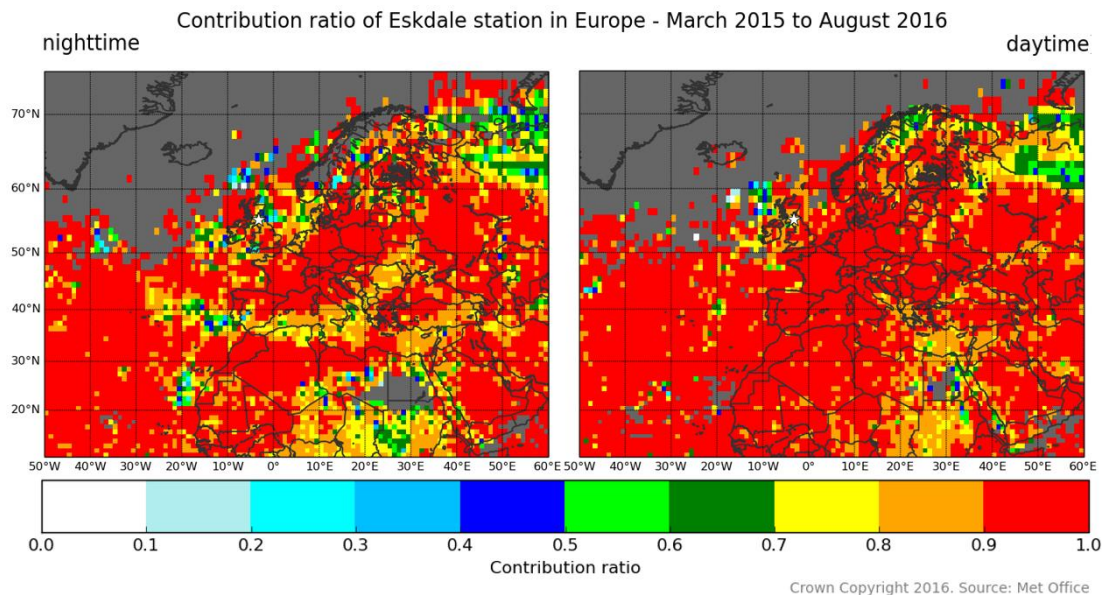
Figure 4.8. The average contribution ratio of Eskdale station in Europe from March 2015 to August 2016 at night (left) and during the day (right).

4.2.3 Norderney station

Norderney station had the average contribution ratio of 88%. Most of its spatial range was characterized by high contribution ratio of 80−100%. The ratio was lower (50−80%) in Central and Southern Africa and also in smaller areas in the central part of North America. Similarly to Payerne, very low (0−50%) contribution ratio occurred in the northeast of Russia and in the southern part of the Pacific Ocean (Fig. 4.9).

Norderney had slightly better contribution ratio at night. The difference was most obvious in South America, Central Africa and northeastern part of Russia where the nighttime contribution ratio was approximately 10% higher compared to daytime (Appendix 6).

For Norderney station clear interference zones occurred both at night and in the daytime. Similarly to Eskdale, there is a third interference zone in the Atlantic Ocean and North Africa at night. The daytime modal interference zone is one of the clearest compared to other stations (Fig. 4.10).
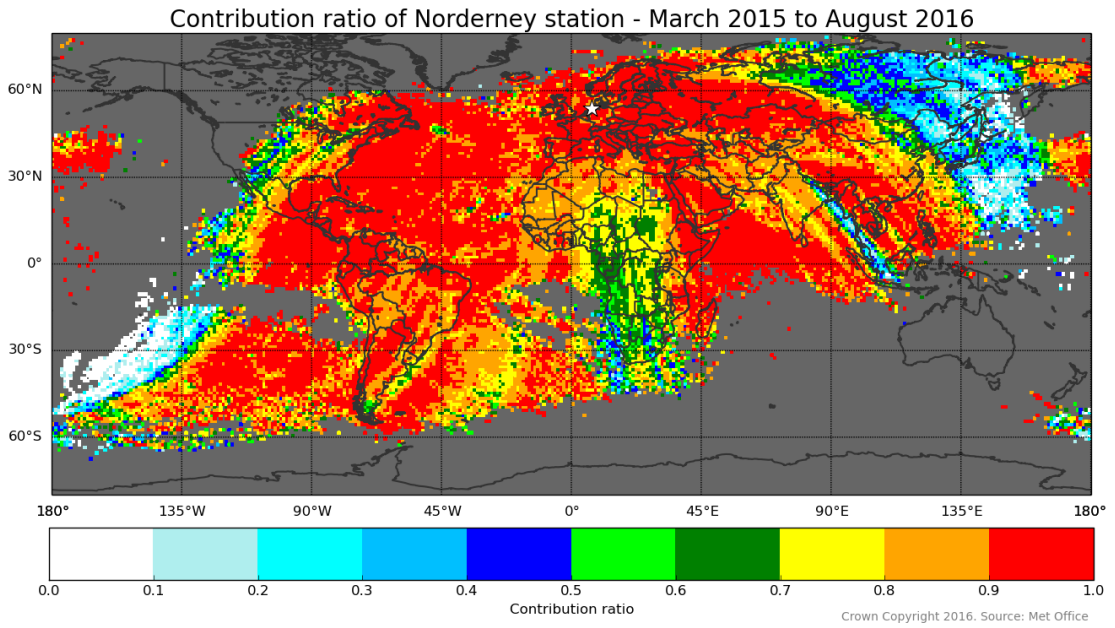
Figure 4.9. The average contribution ratio of Nordernay station from March 2015 to August 2016.
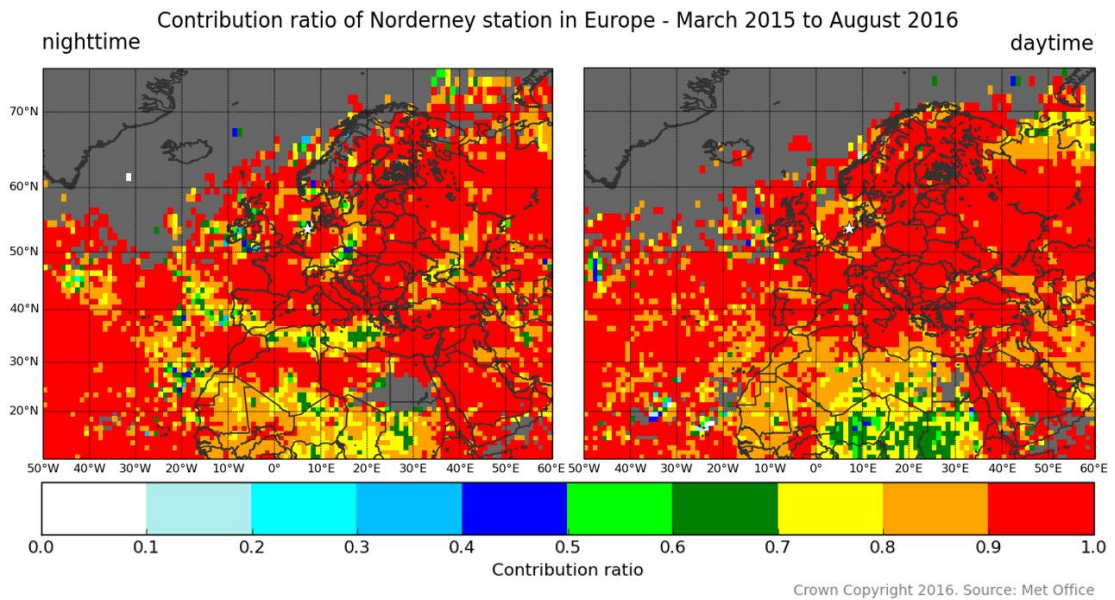

Figure 4.10. The average contribution ratio of Norderney station in Europe from March 2015 to August 2016 at night (left) and during the day (right).

4.2.4 Croatia station

The average contribution ratio of Croatia station was 82%. Over most of its spatial range, Croatia contributed to 70−100% of fixes and in relatively large regions in the eastern part of Russia, in Africa and in the Pacific Ocean the ratio was 90−100%. The largest (compared to other stations rather small) regions with very low (0−30%) contribution occurred in middle of the Pacific Ocean and in the northeast of Russia (Fig. 4.11).

Contribution ratio of Croatia was always better at night with the strongest diurnal difference in Central America and the Atlantic Ocean. In the daytime the station contributed to approximately 30−70% of fixes in the above-mentioned regions whereas at night the ratio was 90−100% (Appendix 7).

Interference zones are also visible. At night, the first zone and parts of the second zone are visible. In addition, a small fragment of the third zone might be identifiable. During the day, the interference zone is harder to see on the map but the contribution ratio clearly decreased from 80−90% to 60−80% in a circular band around the station (Fig. 4.12).
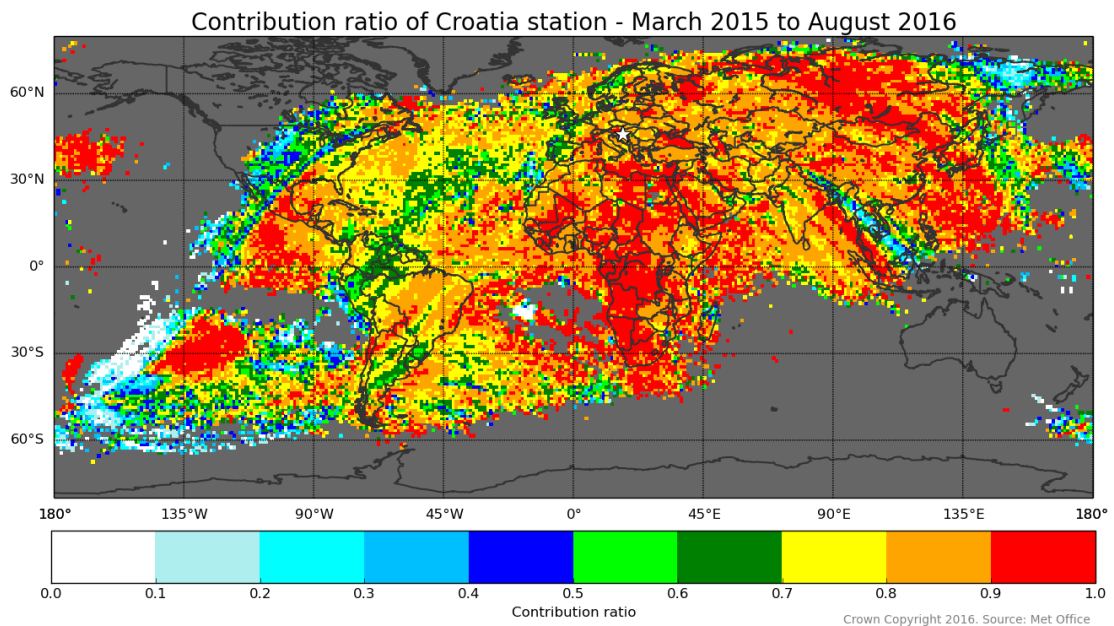

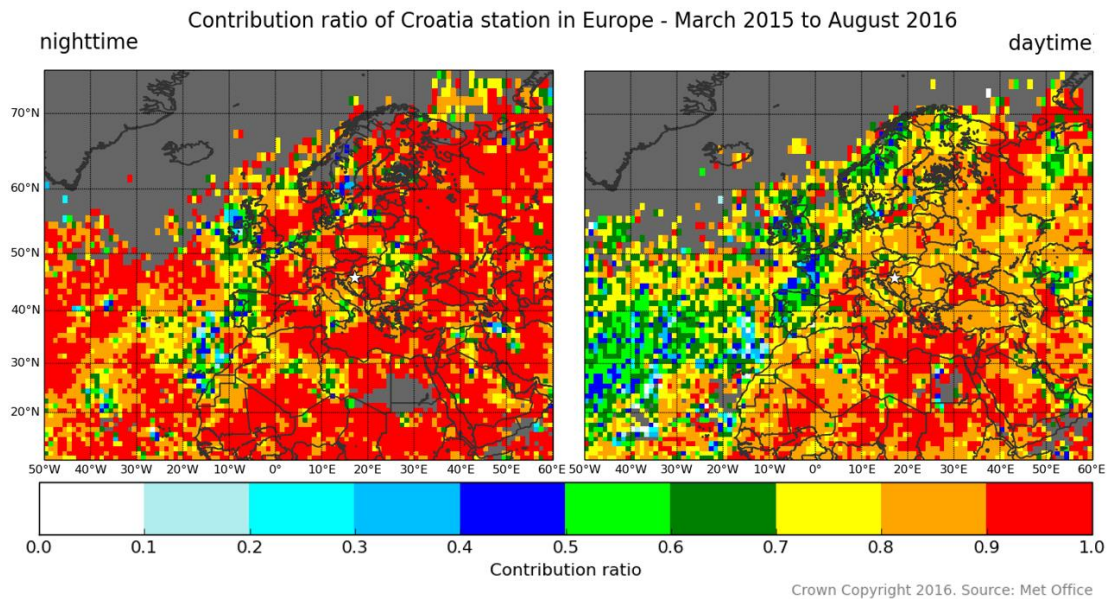Figure 4.11. The average contribution ratio of Croatia station from March 2015 to August 2016.

Figure 4.12. The average contribution ratio of Croatia station in Europe from March 2015 to August 2016 at night (left) and during the day (right).

4.2.5 Exeter station

The contribution ratio of Exeter was clearly higher in the Western Hemisphere, with the highest values in the North Atlantic Ocean, the eastern part of North America, in Central America and in the northern part of South America. An area with 90−100% contribution ratio also extended to the easternmost part of Russia, where Payerne, Norderney and Croatia missed a lot of fixes. Low contribution (0−50%) by Exeter occurred similarly to Eskdale in northwest-southeast directed swath through the eastern part of Asia but covered larger area. In addition, low contribution ratio was observed in the southern part of Africa and along northwest-southeast directed bands from the Middle East to India (Fig. 4.13). The average contribution ratio of Exeter was 78%.

The most obvious difference between day and night occurred in the Middle East and India, where the ratio was approximately 30% higher at night compared to the daytime. In contrast, slight decrease in contribution is visible in Central Africa at night (Appendix 8).

44

Exeter have visible interference zones both at night and in the daytime. In addition, similarly to Eskdale, Norderney and Croatia, Exeter seems to have a third interference zone at night (Fig. 4.14).
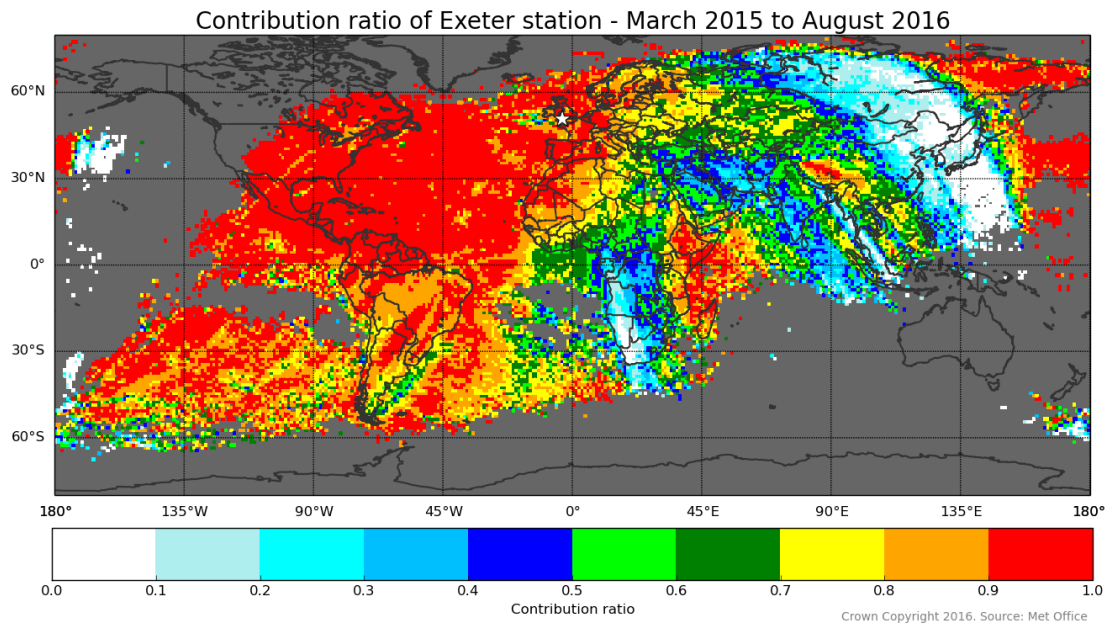

Figure 4.13. The average contribution ratio of Exeter station from March 2015 to August 2016.
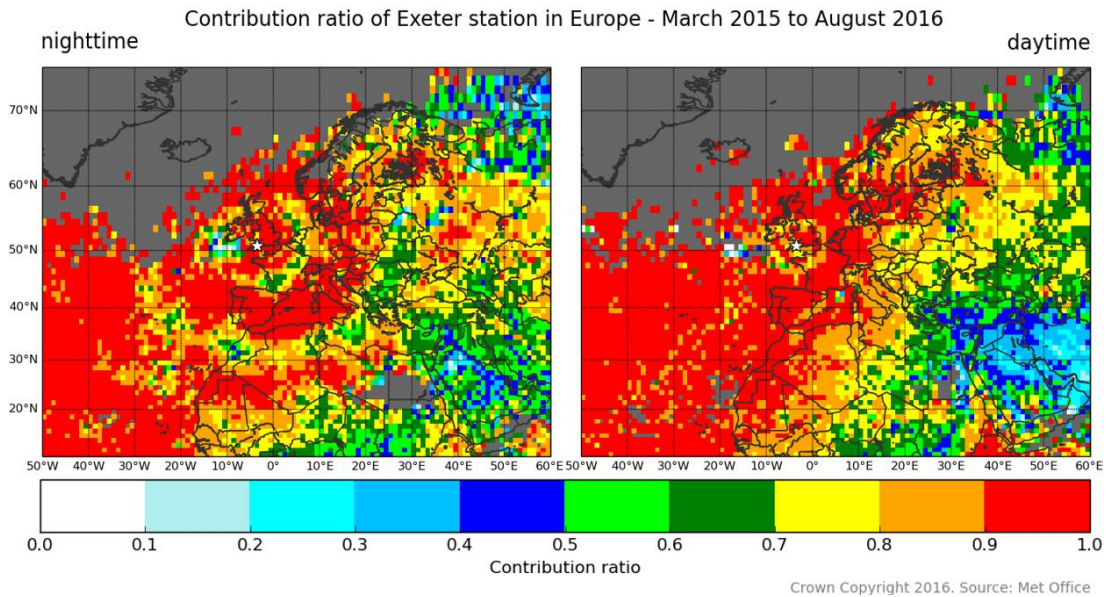
Figure 4.14. The average contribution ratio of Exeter station in Europe from March 2015 to August 2016 at night (left) and during the day (right).

4.2.6 Keflavik station

Keflavik exhibited very high contribution ratio (90−100%) in the northern part of South America, Central America, the eastern part of North America, the Atlantic Ocean, North Europe, and the central and eastern part of Russia. The ratio was clearly lower (0−50%) along a north-south directed swath through Africa and northwest-southeast directed bands from the Middle East to India and Indonesia. The lowest contribution ratio was observed in the central and southern part of the Pacific Ocean where a large area with contribution ratio of 0−10% was found (Fig. 4.15). The average contribution ratio of Keflavik was 73%.

Diurnal differences in the contribution ratio occurred in Southern Europe, North and Central Africa, and Central Asia where the ratio increased by 20−30% at night (Appendix 9). No visible interference zones were observed.
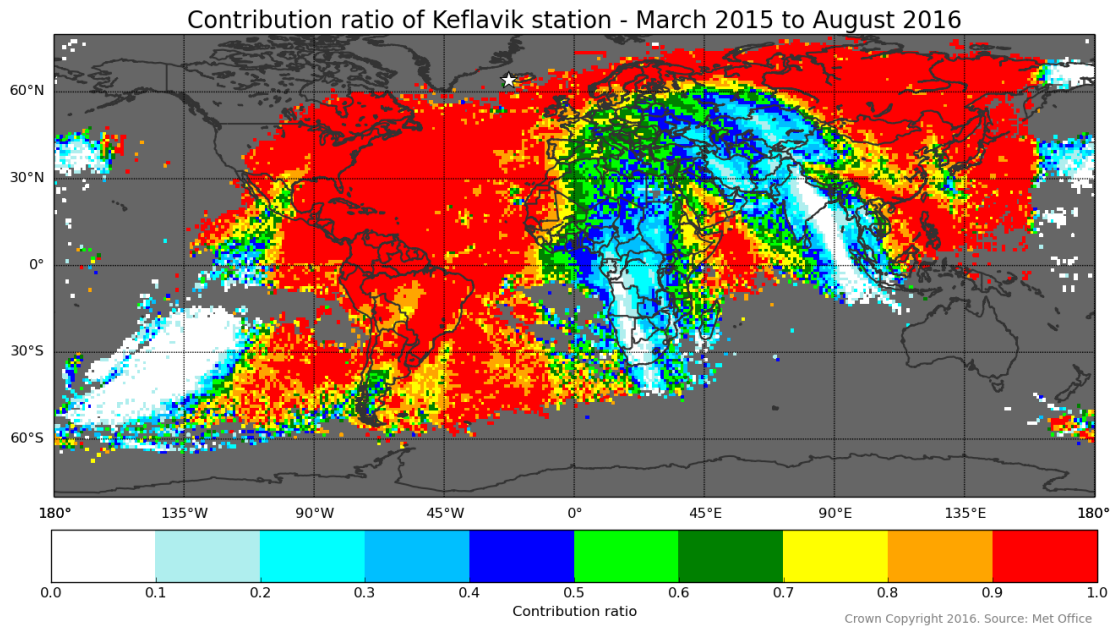
46

Figure 4.15. The average contribution ratio of Keflavik station from March 2015 to August 2016.

4.2.7 Akrotiri station

Akrotiri contributed into 67% of all ATDnet good fixes with highest contribution ratio (90−100%) in most of Africa, the Middle East, and Central and South Asia. Less than 30% of all fixes were detected by Akrotiri in an area from the western part of the North Atlantic Ocean and eastern part of North America to the central part of the Pacific Ocean. In addition, there was a smaller area with low contribution ratio to the southeast of East Asia. Low contribution ratio of 30−40% also occurred in Western and Northern Europe (Fig. 4.16).

The most obvious change in the contribution ratio of Akrotiri between day and night occurred in the central part of the Atlantic Ocean, where the ratio was approximately 30% higher at night. In contrast, the contribution ratio was slightly better during the daytime in Central Asia (Appendix 10).

At night, the first (closest) interference zone is clearly visible whereas only parts of the second interference zone are discernible. The daytime interference zone is not visible (Fig. 4.17).
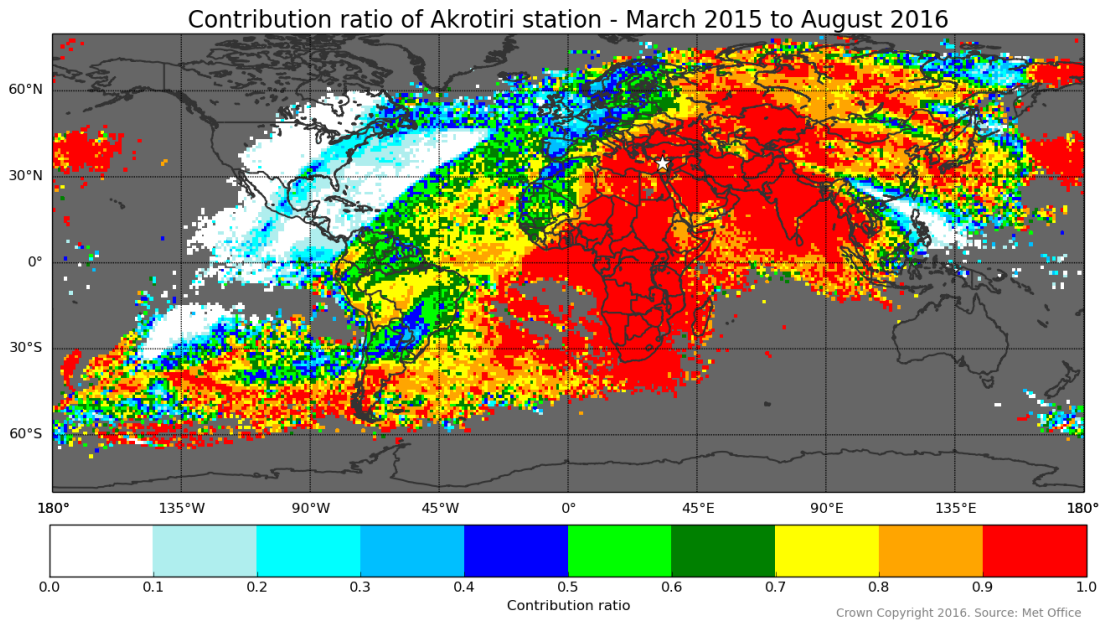
Figure 4.16. The average contribution ratio of Akrotiri station from March 2015 to August 2016.
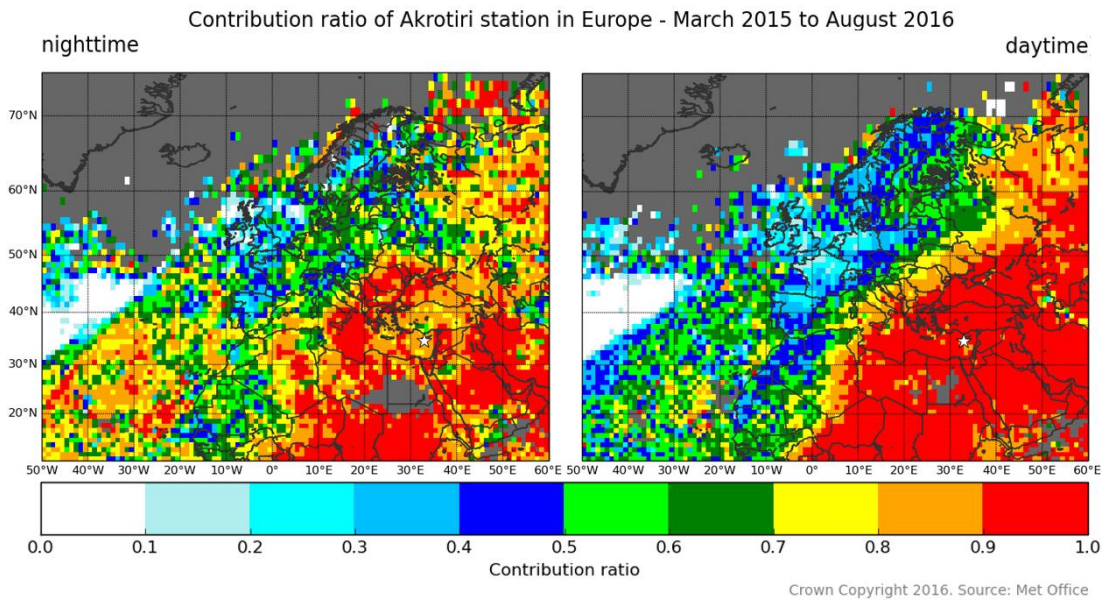

Figure 4.17. The average contribution ratio of Akrotiri station in Europe from March 2015 to August 2016 at night (left) and during the day (right).

4.2.8 Helsinki station

The contribution ratio of Helsinki was clearly better in the Eastern Hemisphere with the peak (90−100%) in the Middle East, India and the northern part of the Indian Ocean. Other areas in this hemisphere had an average contribution ratio of 70−90%. In the Atlantic Ocean and South America, the contribution ratio was on average 40−80%. A northeast-southwest directed area from North America to the South Pacific Ocean was characterized by the lowest contribution ratio of less than 10% (Fig. 4.18). The average contribution ratio of Helsinki was 64%.

Contribution ratio of Helsinki was significantly higher at night in the Atlantic Ocean, South America, Western Europe and Western Africa. The ratio increased by 30−50% compared to the daytime in these areas (Appendix 11). No visible interference zones were observed.
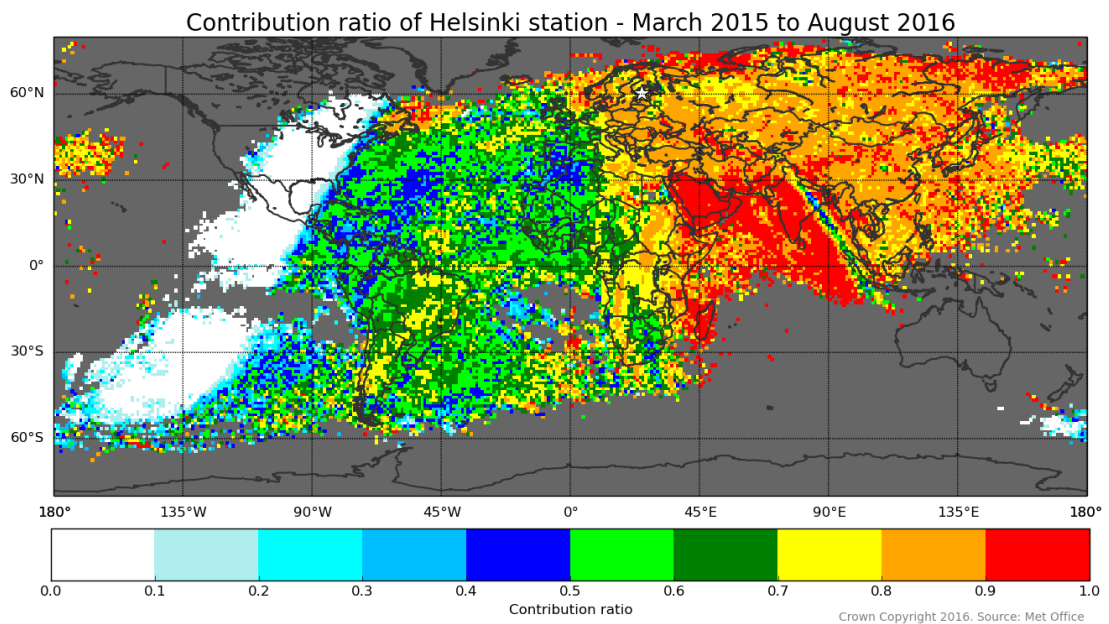

Figure 4.18. The average contribution ratio of Helsinki station from March 2015 to August 2016.

4.2.9 Valentia station

Valentia was characterized by one of the lowest average contribution ratio of 63%. The highest contribution ratio (90−100%) occurred in a northeast-southwest directed area from the North Atlantic Ocean to the central part of the Pacific Ocean. In Europe, the contribution ration dropped from 100% in the west to 50% in the east. Contribution ratio was very low (0−10%) in large northwest-southeast directed areas through East Asia and in the southern part of Africa. In addition, relatively low contribution (10−50%) was observed in Central Africa, the Middle East and India (Fig. 4.19).

Changes in the contribution ratio of Valentia between the day and night occurred in Central Asia, South America and the central part of the Atlantic Ocean. At night, the contribution ratio was approximately 30% higher in Central Asia, and approximately 10% higher in South America and in the central part of the Atlantic Ocean (Appendix 12).

On the nighttime map, the nearest interference zone is visible, but not as clearly as for many other stations. The second interference zone is also visible but harder to distinguish due to relatively strong east-to-west gradient in the contribution ratio in Europe. In the daytime, the contribution ratio was lower around the station, but no clear interference zone was observed (Fig. 4.20).
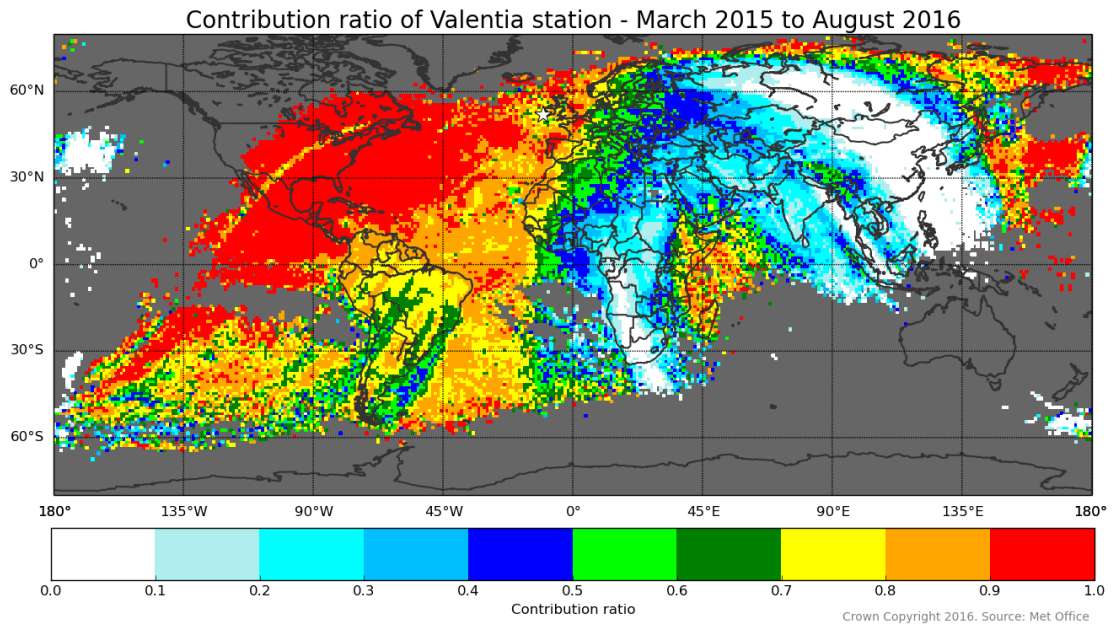
Figure 4.19. Contribution ratio of Valentia station from March 2015 to August 2016.
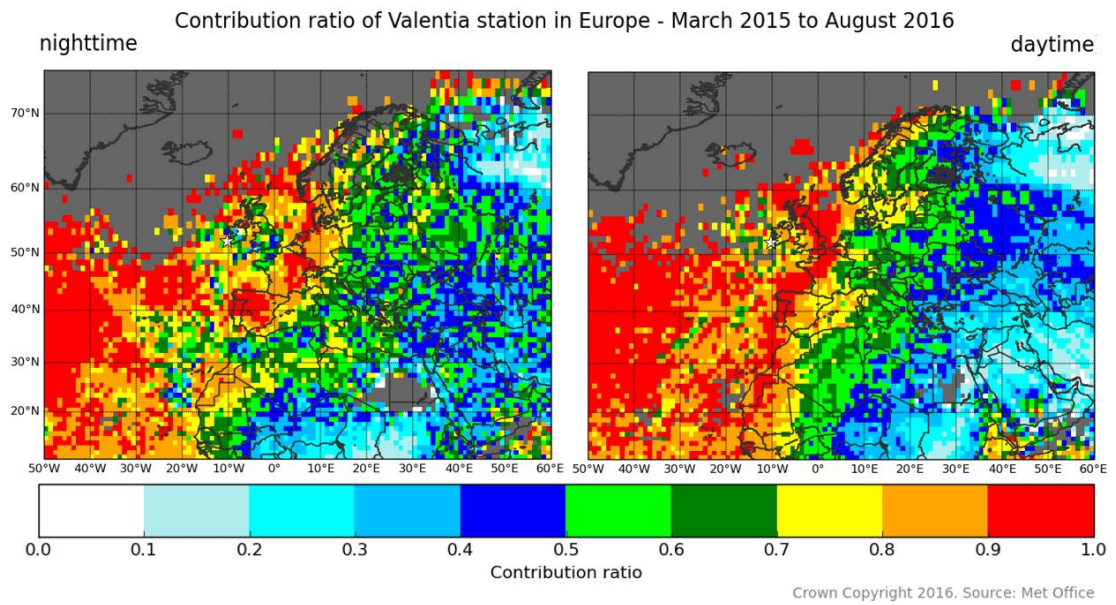

Figure 4.20. The average contribution ratio of Valentia station in Europe from March 2015 to August 2016 at night (left) and during the day (right).

4.2.10 Gibraltar station

Gibraltar was characterized by the lowest average contribution ratio of 43%. Areas with very low contribution ratio (0−10%) encompass almost the whole Asia, Eastern Europe, Central and Southern Africa, and some parts of the South Pacific Ocean. In addition, low contribution (mostly 40−50%) occurred in South America and in parts of the South Pacific Ocean. The best contribution ratio of Gibraltar of 90−100% was observed in a northeast-southwest directed band from North America to the central part of the Pacific Ocean (Fig. 4.21).

No significant differences between day and night were observed for Gibraltar. A bit higher contribution ratio occurred in Asia at night and in South America in the daytime but the difference was only approximately 10% (Appendix 13).

Interference zones of the station occurred on both, nighttime and daytime maps. At night, the contribution ratio dropped from 90−100% to 80−90% in the western part of the first zone and to 20−70% in the eastern part of the zone. The second zone is visible only to the west and southwest of the station. The daytime interference zone is not well discernible on the map, but in fact, near the station the contribution ratio decreased from 80−100% to 50−80% in a circular band (Fig. 4.22).
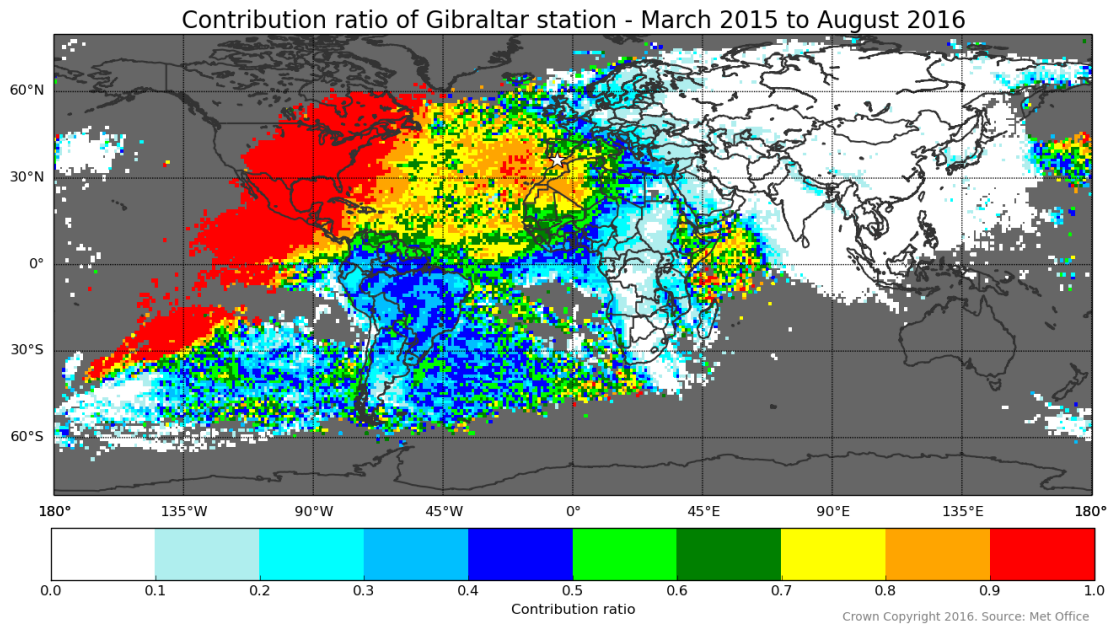
Figure 4.21. The average contribution ratio of Gibraltar station from March 2015 to August 2016.
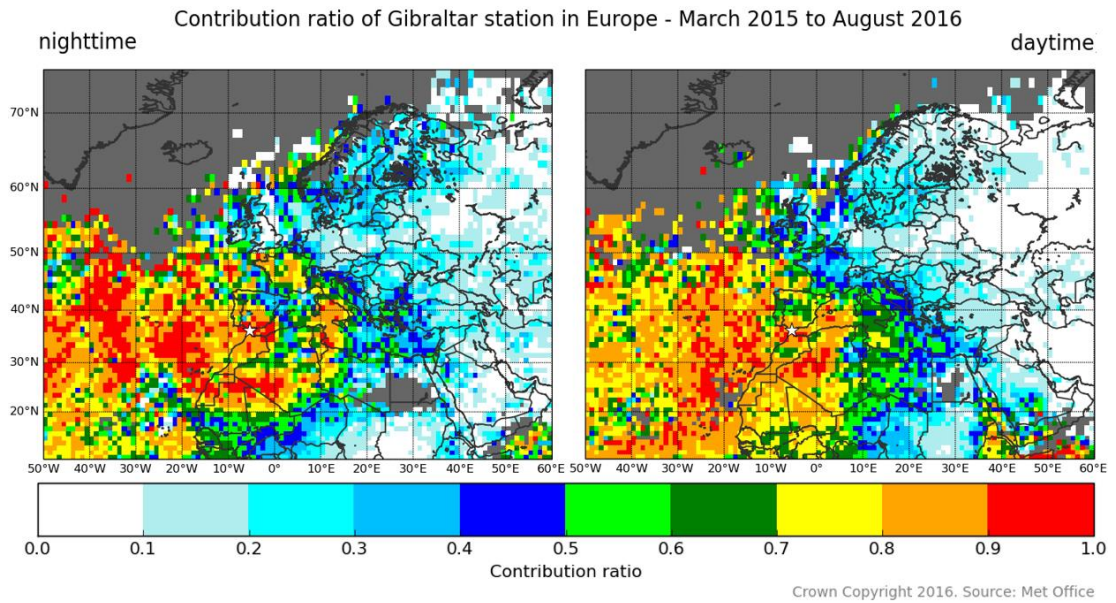

Figure 4.22. The average contribution ratio of Gibraltar station in Europe from March 2015 to August 2016 at night (left) and during the day (right).

4.2.11 Contribution of stations by regions

In Europe, the three stations with the highest contribution ratio were Payerne, Eskdale and Nordernay, which detected 90−100% of all ATDnet good fixes. In addition, Exeter was characterized by high contribution ratio of 70−100%. The weakest contributors were Akrotiri (20−60%) and Gibraltar (0−60%). The latter contributed to less than 30% of fixes in Northern and Eastern Europe.

In North Africa, Payerne was the main contributor. Eskdale, Croatia and Norderney were also characterized by good contribution ratio (80−100%). In addition, Exeter contributed well (80−100%) in the western part and Akrotiri (90−100%) in the eastern part of North Africa. None of the stations had very low contribution ratio all over the region, but the eastern part of North Africa was characterized by low contribution ratio of Keflavik (0−60%), Valentia and Gibraltar (0−50%).

In the North Atlantic Ocean, many stations including Payerne, Eskdale, Norderney, Exeter and Keflavik exhibited very high contribution ratio (90−100%). The situation was similar in the eastern seaboard of North America except that Norderney was worse and Gibraltar much better there. The worst contributors in these regions were Akrotiri and Helsinki, especially in North America (respectively 0−30% and 0−20%).

Payerne and Akrotiri were dominant contributors (90−100%) in Central and Southern Africa, followed by Croatia (80−100%). Keflavik, Valentia (both 0−50%) and Gibraltar (0−30%) were characterized by worst contribution in the region.

In South America, Payerne and Eskdale had very high contribution ratios (90−100%) and Norderney, Keflavik and Exeter also contributed to 80−100% of fixes. The weakest contributor was Gibraltar (20−50%).

Payerne and Eskdale were characterized by the highest contribution ratio (90−100%) in the South Atlantic Ocean where Norderney and Akrotiri also contributed well (70−100%). Croatia was generally as good as Norderney and Akrotiri except that it had a small area in the middle of region with very low contribution ratio. Keflavik

exhibited very high contribution ratio (90−100%) in the eastern part of the South Atlantic Ocean. The worst contributor in the region was Gibraltar (0−60%).

In the South Pacific Ocean, the highest contribution ratio (80−100%) was observed for Payerne, Eskdale and Exeter. In addition, Valentia contributed well with an average contribution ratio of 50−100%. Norderney had high contribution (80−100%) only in eastern part of the South Pacific. All over the area, the lowest contribution ratio of 0−60% had Helsinki. Keflavik and Gibraltar were also characterized by very low contribution in large areas.

In Asia, the best contributors were Akrotiri, Croatia and Helsinki (mostly 80−100% of fixes). Valentia was characterized by low (0−50%) contribution ratio in large areas and the contribution ratio of Gibraltar was nearly zero (0−20%) in the whole Asia.

Table 1. The best and the worst contributing stations by regions.

Region / Contribution	Europe	North Africa	North Atlantic	North America	Central / Southern Africa	South America	South Atlantic	South Pacific	Asia
The best	≥ 90%: Payerne Eskdale Norderney ≥ 70%: Exeter	≥ 90%: Payerne ≥ 80%: Eskdale Croatia Norderney	≥ 90%: Payerne Eskdale Norderney Exeter Keflavik ≥ 80%: Valentia	≥ 90%: Payerne Eskdale Exeter Keflavik Valentia Gibraltar	≥ 90%: Payerne Akrotiri ≥ 80%: Croatia	≥ 90%: Payerne Eskdale ≥ 80%: Norderney Keflavik Exeter	≥ 90%: Payerne Eskdale ≥ 70% Norderney Akrotiri	≥ 80%: Payerne Eskdale Exeter	≥ 80%: Akrotiri Croatia Helsinki
The worst	20–60%: Akrotiri ≤ 60%: Gibraltar		40–70%: Helsinki ≤ 60%: Akrotiri	≤ 30%: Akrotiri ≤ 20%: Helsinki	≤ 50%: Keflavik Valentia ≤ 30%: Gibraltar	20–50%: Gibraltar	≤ 60%: Gibraltar	≤ 60%: Helsinki	≤ 50%: Valentia ≤ 20%: Gibraltar

4.2.12 Monthly contribution ratios

The average monthly contribution ratios of individual stations throughout the study period are presented in Fig. 4.23. This figure compares the operational stability of different stations.

Payerne showed the highest and the most stable contribution ratio. All other stations exhibited major or minor fluctuations. Strongest fluctuations occurred in the contribution ratio of Gibraltar, which was also the worst contributor.
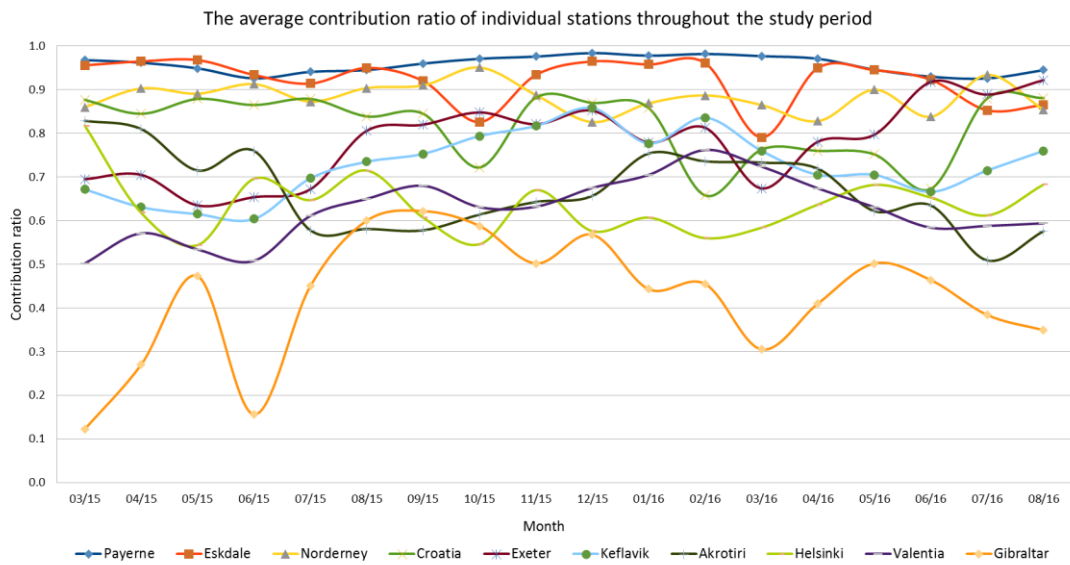

Figure 4.23. The average contribution ratio of individual stations throughout the study period.

5. DISCUSSION

The results revealed significant spatial variations in the average number of contributing stations. The main area with high number of contributing stations occurred in the Atlantic Ocean. This area was characterized by high contribution ratio probably due to stronger flashes and more powerful sferics over the oceans (e.g. Said *et al.* 2013). In addition, propagation losses are smaller over salty water due to higher air conductivity (Wait and Spies 1965). Thus, sensors in the western part of the network receive stronger waveforms with minimal distortion if a flash is located in the Atlantic. To reach the easternmost inland sensors such as Helsinki and Croatia, sferics from the Atlantic still have to travel some distance over land, where conductivity is lower and attenuation higher (Wait and Spies 1965). In addition, it is found that inhomogeneous ground, such as a long stretch of sea and a short section of land, reduces all VLF propagation path when the foreground is poorly conducting (Wait 1965). However, the reason why the number of contributing stations per grid cell never got to 10 or nearly 10 may just be caused by some stations with noise issues (e.g Gibraltar and Helsinki).

High number of contributing stations over the Atlantic is in line with observed higher ATDnet DE there (Enno *et al*. 2016b). This supports the idea that both findings result from stronger lightning and better propagation conditions over the oceans.

As all operational ATDnet sensors are located in and around Europe, it might be expected that the highest number of contributing stations occurs in this area. However, results revealed that the average number of contributing stations was 6−8 in Europe. The visible modal interference zones around most stations definitely contributed to the reduction of the number of contributing stations in Europe. However, the main reason might be in the fact that within the perimeter of the network, weaker lightning and a lot of cloud lightning is detected (Enno *et al*. 2016a). Those sferics are detectable only within relatively short distance from lightning locations (1000−1500 km). In Europe, ATDnet sensor density is high enough to detect such fixes. However, it is very likely

that some more distant (Keflavik, Akrotiri) or noisy (Gibrlatar) sensors do not detect such fixes. This lowers the average number of contributing sensors in Europe.

It has been also shown that despite of somewhat lower average number of contributing stations in Europe, DE and LA are highest there. For example, median location error is found to be no larger than 7.5 km in Europe (Bennet *et al*. 2010a; Poelman *et al.* 2013). At the same time, the number of contributing stations is higher in South America, but median location error is 21 km in Brazil (Bennet *et al.* 2010a). In that case, worse LA is not attributable to low number of contributing stations, but shallow hyperbola intersection angles due to geometry of the network.

Higher than 7 contributing stations in some regions outside the perimeter of ATDnet such as the northwestern part of Africa, South-America and eastern part of North America is probably related to the fact that in distant regions only the most powerful lightning is detected. In addition to powerful sferics, emissions that originate from the Americas propagate mostly over the ocean, which is characterized by lower attenuation of the waves. For very distant regions, the distance between a fix and the center of ATDnet is much bigger than the diameter of ATDnet. Thus, sferics that are strong enough to be detected by the closest sensor(s) are also likely detectable to many other sensors.

The average number of contributed stations was generally lower to the east and south of Europe. Lower number of contributing stations in Asia and southern Africa may be related to generally weaker lightning over land (e.g. Said *et al.* 2013). Potentially even more important is the previously mentioned fact that continental propagation paths are less conductive and thus losses and distortion are much higher (Wait and Spies 1965). The conductivity is especially low over deserts, thus the Sahara desert is expected to substantially affect propagation from central and southern Africa.

Two additional areas with interesting but less reliable results were found. The largest area with more than 9 contributing stations in the northwestern part of the Indian Ocean probably results from detection of only a small number of very strong lightning

discharges. It was demonstrated that the area disappeared if the minimum number of ATDnet fixes per grid cell was increased from 10 to 100 (Appendix 14). This indicates that ATDnet DE is low in the Indian Ocean and probably only the strongest fixes that are seen by most of the stations are detected. This agrees with low ATDnet DE relative to LIS in the Indian Ocean found by Enno *et al.* (2016b). In addition, the region is characterized generally lower lightning activity accordingly to LIS observations (Albrecht *et al*. 2016).

The other interesting area encompasses the southern part of the Pacific Ocean and is characterized by the lowest number of contributing stations. It is assumed to be mainly caused by misplaced European fixes as it is the antipode of Europe. In the fix location procedure the system has to decide between two possible locations on the opposite sides of the world. In case of a limited number of contributing stations it is more likely that a wrong decision is made and a European fix is misplaced to the South Pacific Ocean. Most of the area disappeared if the minimum number of fixes per grid cell was increased from 10 to 100 (Appendix 14).

Diurnal changes in the average number of contributing stations were rather small with slightly higher number of contribution stations at night in most of the spatial range of ATDnet. The higher number of contributing stations in the Atlantic Ocean at night is probably not related to lightning properties, which are assumed to have no diurnal cycle over the oceans. The reason might rather result from stronger skywaves due to better reflection conditions from ionosphere at night (Chapman and Pierce 1957).

The higher number of contributing stations at night also occurred in Europe, where it was more surprising because of stronger modal interference and overlapping interference zones. However, decrease in contribution ratios and areas of interference zones were relatively small. The result may be related to the fact that ATDnet quality control rejects many fixes in Europe at night due to distorted waveforms (Gaffard *et al*. 2008). Therefore, only the strongest sferics emitted by strong lightning discharges and often detected by many stations result in good fixes. This assumption could be checked in another study by using not only good but also poor fix data.

The only region with higher number of contributing stations during the day was Southern Africa. This might occur due to higher flash rate and larger number of strong flashes during the day in Africa (Blakeslee *et al.* 2014), which coincides with day in Europe.

Seasonal changes in the number of contributing stations were generally small. The biggest change was observed in the middle of the Atlantic Ocean, where the number of contributing stations dropped from 8−9 to 5−6 in spring. Areas with lower number of contributing stations in spring disappeared if the minimum number of fixes per grid cell was increased from 10 to 100 (Appendix 15). This indicates that the finding is not reliable as only a limited number of fixes was registered in the middle of Atlantic Ocean in spring. Moreover, as the average number of stations per fix is low it might be that the fixes actually occurred elsewhere and were wrongly located to this area due to lack of contributing stations. This idea is also supported by previously observed tendency of the operational ATDnet to produce spurious fixes in parts of the North Atlantic Ocean (Enno, personal communication, 28.04.2017).

As some of the results were found to be unreliable because of low number of fixes, it is appropriate to mention that the minimum number of 10 fixes per grid cell was initially chosen to check the areas at the edge of the ATDnet spatial range. As such areas often have a limited number of detected fixes it is reasonable to use a small fix threshold at first and later check the results with higher threshold if needed.

Slightly higher number of contributing stations in the Atlantic Ocean and Europe in winter may result from relatively higher frequency of stronger positive CG lightning in winter (Rakov 2003). However, more investigation is needed to check this assumption.

The average contribution ratios of individual stations revealed the best and the worst operational stations. Contribution ratios of Payerne, Eskdale and Norderney were the highest. These stations had been free from disruptive noise issues. In addition, Payerne

is located high in Switzerland which is the advantages for detecting an electromagnetic waves.

A few small areas with lower contribution ratio in these stations can be explained by the configuration of the network. Areas with near-zero contribution ratio agree with the typical shape of network blind spots. A network blind spot is a distant area where certain combinations of a reference station and other stations cannot be used as resulting time difference values would be unacceptably high for the current system. The location of the blind spot for a given station depends on the combination of stations. Clear lower contribution area refers that within the spot mostly combinations of stations that leave the station 'blind' are used. In addition, Croatia station contributed well, but the average contribution was a little lower with no certain blind spots.

Exeter, Helsinki and Valentia stations are known to have certain problems during the study period, which lower the contribution ratio. For example, at beginning of the study period Exeter had problems with solar panels, which are source of interference for ATDnet sensors. In May 2016, the station was moved away from the solar panels, which may explain the improvement in its performance at the end of the study period (Fig. 4.23). In August 2015, solar panels and invertors were installed to the roof of the Finnish Meteorological Institute where an ATDnet sensor is located. This resulted in increased interference and lower contribution ratio. Interference was tried to mitigate by applying notch filters but no clear improvement in the contribution ratio can be seen. In addition, Valentia station with low average contribution ratio is known to suffer from electrical/earthing noise from the installation set up, which again results in lower contribution (Odams, personal communication, 24.01.17).

Gibraltar was characterized by the worst contribution ratio. Although Gibraltar is one of the closest stations to Africa, it does not contribute much there. This shows that the quality of a station might be more important in certain situations than the distance of the station from a region. It can be seen that Gibraltar has not only low contribution ratio but also big fluctuations in the contribution ratio, which are especially obvious at

the beginning of the study period (Fig. 4.23). Low contribution ratio in March 2015 resulted from the fact that the station was not fully upgraded yet. The dip after May 2015 is attributable to an intermittent problem of GPS 'seeing' not enough satellites at times. The issue was resolved in July 2015 with a shorter GPS cable leading to better quality of GPS signal (Odams, personal communication, 24.01.17). This study revealed that despite of solving the timing problem the sensor still have major issues which should be investigated and dealt with in order to improve the network.

Keflavik and Akrotiri had lower contribution ratio in Europe although they have been free of major technical issues. Their contribution ratio is lower probably because both are locate relatively far from the network center which prevents them registering IC and weaker CG lightning.

It has been noticed that easternmost stations, such as Akrotiri, Croatia and Helsinki contribute the best in Asia. Wait (1965) suggested that a significant amount of energy is converted to the higher modes at sea-land transition. As higher modes of skywave weaken faster, it might be one of the reason, why the easternmost stations contribute better in Asia compared to Atlantic.

Clearly visible circular areas with dropped contribution ratio around most stations confirm the detrimental effect of modal interference on ATDnet. Similarly to Gaffard *et al*. (2008) and Bennet *et al.* (2011) the main modal interference zones found in the present study are located approximately ~450 km from stations during the day and ~600 km and ~2100 km from stations at night.

In addition, for Eskdale, Norderney, Croatia and Exeter stations, parts of an additional interference zone were visible at night. This interference zone is similar to dropped signal-to-noise ratio approximately 3600 km from stations found in the two earlier studies mentioned above (Gaffard *et al.* 2008; Bennet *et al.* 2011). Furthermore, weaker contribution ratio areas nearby some stations were observed at night. These may correspond to a narrow band of reduced waveform correlation ~300 km from stations found by Gaffard *et al*. (2008), Bennet *et al.* (2011) and Hudson (2014).

Hudson (2014) found the nearest minimum in signal to noise ratio to be located ~300 km from stations at night corresponding to the interference between the ground wave and the first order skywave. Second and greater drop of signal-to-noise ratio was located approximately 600 km from sensors, which is very similar to the location of the first obvious interference zone found in the present study. Interestingly, Hudson (2014) did not observe the interference zone at 2100 km from stations that was obvious in the present study. In contrast, Gaffard (2008) and Bennet *et al*. (2011) observed both, the 600 km and 2100 km nighttime interference zones. Differences between individual analyses indicate that further, more detailed, study is needed to get a complete picture of all potential modal interference zones.

Interference zones were not clearly visible for some stations like Helsinki and Akrotiri during the day. To check if the zones were completely missing or simply too weak to be discernible with the used color scale, new maps with 2% contribution ratio color bins were prepared. Results revealed a very weak interference zone around Akrotiri during the day (Appendix 16). Maps of Helsinki remained noisy without any clear interference zones. The only observation is lower contribution very close to the station (Appendix 17). Theoretically, interference zones should occur for every station. Thus, their absence indicates that there might be other issues that have greater impact on DE than the modal interference. As mentioned before, at Helsinki station, solar panels caused radio noise that was probably strong enough to hide the effect of modal interference.

In addition, interference zones of Keflavik were not visible. They are expected to be located in the North Atlantic where the lightning activity is too low (below 10 fixes per grid cell) for actually observing them.

CONCLUSION

The present study investigated the number of contributing stations and contribution ratios of individual stations in the spatial range of ATDnet during March 2015 to August 2016.

The highest number of contributing stations per lightning event occurred in Atlantic Ocean with an average of 8−9 contributing stations. In Europe, the average number of contributing stations was 6−8. The number of contributing stations decreased relativity fast in land areas to the east and south of the network perimeter but maintained its high value or even increased slightly in the Atlantic Ocean to the west of the network. The lowest average number of stations of 4−6 contributing stations per fix was observed in the South Pacific Ocean, which is the antipode of Europe.

The results clearly indicate that differences in air conductivity make ATDnet more sensitive to oceanic lightning and less sensitive to continental lightning. Thus, for better DE and LA in continental areas, such as Africa and Asia, a number of sensors need to be installed there. In contrast, lower sensor density should be sufficient to detect a significant fraction of lightning over the oceans.

Significant differences between contribution ratios of individual stations were observed. The best station Payerne contributed to 96% of all ATDnet good fixes whereas the worst station Gibraltar contributed to only 43% of the fixes. Other very good contributors were Eskdale and Norderney and very poor contributors included Helsinki and Valentia. For many stations with lower contribution ratio, there were large areas with almost no detection. The results could be used for improving the network without adding new stations. The sites of the best contributors should be investigated to determine the properties of an ideal ATDnet sensor site. This information could then be used to relocate worse stations.

Seasonal changes in the number of contributing stations and contribution ratios were very small. Diurnal changes where somewhat larger with the average number of contributing stations higher at night.

Another important finding was the existence of circular modal interference bands with lower contribution ratio around many ATDnet stations. During the day one clear interference zone approximately 450 km from stations was observed. At night, there were two clearly visible interference zones located approximately 600 and 2100 km from stations. A more detailed study is needed to clarify the spatial characteristics of the zones. In the future, it would be rational to optimize the locations of sensors so that areas with multiple overlapping interference zones are avoided as much as possible.

The overall results of the current thesis contribute significantly to ATDnet research and development. The assessment of the network on the station level revealed some problematic areas where only a limited number of ATDnet sensors are useable. It also suggested that some of the current sensors need to be moved to betters sites. Those findings are very useful in the ongoing planning process of the new more accurate and efficient ATDnet next generation.

RESÜMEE

Käesolev magistritöö uuris registreerimises osalenud detektorite arvu ja üksikute detektorite panustamissuhte ruumilist jagunemist välgudetektorite võrgustikus ATDnet uurimisperioodil märts 2015 kuni august 2016.

Kõrgeim registreerimises osalenud detektorite arv ühe välgusündmuse kohta esines Atlandi Ookeanil, kus registreerimises osales keskmiselt 8−9 detektorit. Euroopas oli keskmine registreerimises osalenud detektorite arv 6−8. Detektorite arv vähenes suhteliselt kiiresti maismaa aladel Euroopast ida ja lõuna suunas, kuid püsis kõrge või isegi kasvas veidi detektoritest läänes asuva Atlandi ookeani kohal. Madalaim keskmine registreerimises osalenud detektorite arv esines Euroopa suhtes teisel pool maakera asuvas Vaikse ookeani lõunaosas, kus välgusündmust registreeris keskmiselt 4−6 detektorit.

Tulemused näitavad selgelt, et erinevused õhu elektrijuhtivuses muudavad ATDnet'i tundlikumaks ookeani kohal esinevate välkude suhtes ja vähem tundlikuks maismaa välkude suhtes. Sellest tulenevalt oleks vajalik Aafrika ja Aasia maismaa-aladele paigaldada mitmeid detektoreid, et parandada sealset registreerimisefektiivsust ja asukohatäpsust. Madalam detektorite tihedus peaks aga olema piisav, et registreerida märkimisväärne osa äikesest ookeanite kohal.

Tulemustest selgus märkimisväärsete erinevuste esinemine detektorite panustamissuhetes. Parim detektor Payerne registreeris 96% kõikidest ATDnet'i hea kvaliteediga välgusündmustest, samal ajal kui nõrgim detektor Gibraltar registreeris ainult 43% välgusündmustest. Teised väga head panustajad olid Eskdale ja Norderney ning nõrgalt panustasid veel Helsingi ja Valentia. Paljud nõrkade panustamissuhetega detektorid ei registreerinud suurtel aladel peaaegu üldse. Uurimistöö tulemust saab kasutada, et täiendada praegust võrgustikku detektorite arvu suurendamata. Parimate detektorite asukohti uurides saab kindlaks teha ideaalsete paikade omadused ning selle teadmise põhjal paigutada ümber töös avaldunud nõrgemad detektorid.

Sesoonsed muutused registreerimises osalenud detektorite arvus ja panustamissuhetes olid väga väikesed. Ööpäevased muutused olid mõnevõrra suuremad – paljudes piirkondades oli registreerinud detektorite keskmine arv öösel ligikaudu ühe võrra suurem.

Tähtis tulemus oli ka ringjate modaalse interferentsi alade esinemine madalama panustamissuhtena ümber mitmete ATDnet'i detektorite. Päeval esines üks selge interferentsi tsoon ligikaudu 450 km detektorist. Öösel oli tsoone kaks ja need asusid ligikaudu 600 km ja 2100 km kaugusel detektorist. Detailsem uuring on vajalik, et selgitada välja tsoonide ruumilised omadused. Tulevikus on mõistlik muuta detektorite asukohti nii, et mitmete interferentsi tsoonide kattumine oleks välditud nii palju kui võimalik.

Käesoleva töö tulemused aitavad märkimisväärselt kaasa ATDnet'i teadus- ja arendustegevusele. Võrgustiku hindamine detektorite tasandil avalikustas probleemsed alad, kus ainult limiteeritud arv ATDnet'i detektoreid panustab välkude registreerimisse. Lisaks on soovitatav, et mõned praegused detektorid paigaldatakse parematesse asukohtadesse. Tulemusi kasutatakse käimasoleva ATDneti'i järgmise põlvkonna välgudetektorite võrgustiku planeerimisel ja arendamisel.

LIST OF REFERENCES

Albrecht, R. I., Goodman, S. J., Buechler, D. E., Blakeslee, R. J. and Christian, H. J., 2016. Where are the lightning hotspots on Earth?. *Bulletin of the American Meteorological Society,* 97(11):2051−2068.

Bennett, A. J. 2011. Comparison between the UK Met Office ATDnet and the WWLLN lightning location networks in the Tropical North Atlantic during January and June 2010. Internal Report. Met Office, Exeter, UK.

Bennett, A. J., Atkinson, N. and Kyle, E. 2010a. Study on potential synergy of global scale ATDnet measurements and the MTG LI. Final report for a EUMETSAT study, EUM/CO/09/4600000704/KJG. Met Office, Exeter, UK.

Bennett, A. J., Callaghan, G., Gaffard, C., Nash, J. and Smout, R. 2010b. The effect of changes in lightning waveform propagation characteristics on the UK Met Office long range lightning location network (ATDnet). 21st International Lightning Detection Conference. Orlando, USA, 19−20 April.

Bennett, A. J., Gaffard, C., Nash, J., Callaghan, G. and Atkinson, N. C. 2011. The effect of modal interference on VLF long-range lightning location networks using the waveform correlation technique. *Journal of Atmospheric and Oceanic Technology*, 28(8):993−1006.

Blakeslee, R. J., Mach, D. M., Bateman, M. G. and Bailey, J.C. 2014. Seasonal variations in the lightning diurnal cycle and implications for the global electric circuit. *Atmospheric Research,* 135:228−243.

Boccippio, D. J., Koshak, W. J. and Blakeslee, R. J. 2002. Performance assessment of the optical transient detector and lightning imaging sensor. Part I: Predicted diurnal variability. *Journal of Atmospheric and Oceanic Technology*, 19(9):1318−1332.

Budden, K. G. 1957. The" Waveguide Mode" Theory of the Propagation of Very-Low-Frequency Radio Waves. *Proceedings of the IRE*, 45(6):772−774.

Chapman, J. and Pierce, E. T. 1957. Relations between the character of atmospherics and their place of origin. *Proceedings of the IRE*, 45(6):804−806.

Colin, R. I. 1970. Dr. Meint Harms and Hyperbolic Navigation a Vignette of Radio Navigation History. *IEEE Transactions on Aerospace and Electronic Systems*, 1:2−9.

Cummins, K. L. and Murphy, M.J. 2009. An overview of lightning locating systems: History, techniques, and data uses, with an in-depth look at the US NLDN. *IEEE Transactions on Electromagnetic Compatibility*, 51(3):499−518.

Cummins, K. L., Murphy M. J. and Tuel J. V. 2000. Lightning detection methods and meteorological applications. *IV International Symposium on Military Meteorology*: 26−28.

Enno, S.-E. Scientist at the Met Office, Observations R&D. Personal communication. (28.04.2017).

Enno, S.-E., Anderson, G. and Sugier, J. 2016a. ATDnet detection efficiency and cloud lightning detection characteristics from comparison with the HyLMA during HyMeX SOP1. *Journal of Atmospheric and Oceanic Technology*, 33(9):1899−1911.

Enno, S.-E., Rudlosky, S., Sugier, J. and Labrador, L. 2016b. Comparison and characterisation of ATDnet versus LIS for the period of 2008 to 2014. Final report for a EUMETSAT study, EUM/CO/15/4600001643/KJG. Met Office, Exeter, UK.

Finke, U. and Hauf, T. 2002. Detect and locate lightning events from geostationary satellite observations, report part 2: Feasibility of lightning location from a geostationary orbit. Technical Report, EUM/CO/02/1016/SAT. Leibniz University of Hanover, Hanover, Germany.

Gaffard, C., Nash, J., Atkinson, N., Bennett, A., Callaghan, G., Hibbett, E., Taylor, P., Turp, M. and Schulz, W. 2008. Observing lightning around the globe from the surface. 20th International Lightning Detection Conference. Tucson, Arizona, USA, 24−25 April.

GHRC (Global Hydrology Resource Center). Space Research and Observations. Lightning Imaging Sensor (LIS) Overview (homepage). https://lightning.nsstc.nasa.gov/lis/overview_lis_instrument.html (11.04.17).

Goodman, S. J., Blakeslee, R. J., Koshak, W. J., Mach, D., Bailey, J., Buechler, D., Carey, L., Schultz, C., Bateman, M., McCaul, E. and Stano, G. 2013. The GOES-R geostationary lightning mapper (GLM). *Atmospheric Research*, 125:34−49.

Hudson, T. S. 2014. Lightning Atmospheric Propagation Model for ATDnet. Technical Report. Met office, Exeter, UK.

Kikuchi, T. 1986. Waveguide model analyses of Omega VLF wave propagation at 13.6 kHz. *Journal of Atmospheric and Terrestrial Physics,* 48(1):15−23.

Krider, E. P., Noggle, R. C. and Uman, M. A. 1976. A gated, wideband magnetic direction finder for lightning return strokes. *Journal of Applied Meteorology*, 15(3):301−306.

Krider, E. P., Noggle, R. C., Pifer, A. E. and Vance, D. L. 1980. Lightning direction-finding systems for forest fire detection. *Bulletin of the American Meteorological Society*, 61(9):980−986.

Lee, A. C. L. 1986. An Operational System for the Remote Location of Lightning Flashes Using a VLF Arrival Time Difference Technique. *Journal of Atmospheric and Oceanic Technology*, 3(4): 630–642.

Lewis, E. A., Harvey, R. B. and Rasmussen, J. E. 1960. Hyperbolic direction finding with sferics of transatlantic origin. *Journal of Geophysical Research*, 65:1879–1905.

Lojou, J.-Y., Murphy, M. J., Holle, R. L. and Demetriades, N. W. S. 2009. Nowcasting of thunderstorms using VHF measurements. *Lightning: Principles, Instruments and Applications*: *review of modern lightning research.* Edited by Betz H.D., Schumann U. and Laroche P. Berlin: Springer Science & Business Media, 253−270.

Nag, A., Murphy, M. J., Schulz, W. and Cummins, K. L. 2015. Lightning locating systems: Insights on characteristics and validation techniques. *Earth and Space Science*, 2:65–93.

Odams, P. ATDnet Network Specialist. Personal communication. (24.01.17).

Poelman, D. R. 2010. On the Science of Lightning: An Overview. *Wetenschappelijke en technische publicatie*, 56.

Poelman, D. R., Honoré, F., Anderson, G. and Pedeboy, S. 2013. Comparing a regional, subcontinental, and long-range lightning location system over the Benelux and France. *Journal of Atmospheric and Oceanic Technology,* 30:2394–2405.

Rakov, V. A. 2003. A review of positive and bipolar lightning discharges. *Bulletin of the American Meteorological Society*, 84(6):767−776.

Rakov, V. A. and Uman, M. A. 2003. *Lightning: Physics and Effects*. Cambridge: Cambridge University Press.

Said, R. K., Cohen, M. B. and Inan, U. S. 2013. Highly intense lightning over the oceans: Estimated peak currents from global GLD360 observations. *Journal of Geophysical Research: Atmospheres,* 118(13):6905−6915.

Smith, M. 2017. Flashy first images arrive from NOAA's GOES-16 Lightning Mapper. NASA (National Aeronautics and Space Administration) (homepage). https://www.nasa.gov/feature/goddard/2017/flashy-first-images-arrive-from-noaa-s-goes-16-lightning-mapper (11.04.2017).

Thompson, K. B., Bateman, M. G. and Carey, L. D. 2014. A comparison of two ground-based lightning detection networks against the satellite-based Lightning Imaging Sensor (LIS). *Journal of Atmospheric and Oceanic Technology*, 31(10):2191−2205.

Volland, H. 1995. Longwave sferics propagation within the atmospheric waveguide. *Handbook of Atmospheric Electrodynamics* (Vol. 2). Edited by Volland, H. Boca Raton: CRC Press, 65−90.

Wait, J. R. 1965. Influence of an inhomogeneous ground on the propagation of VLF radio waves in the earth-ionosphere waveguide. *Radio Science*, 69:969−975.

Wait, J. R. and Spies, K. P. 1965. Influence of finite ground conductivity on the propagation of VLF radio waves. *Radio Science*, 69:1359−1373.
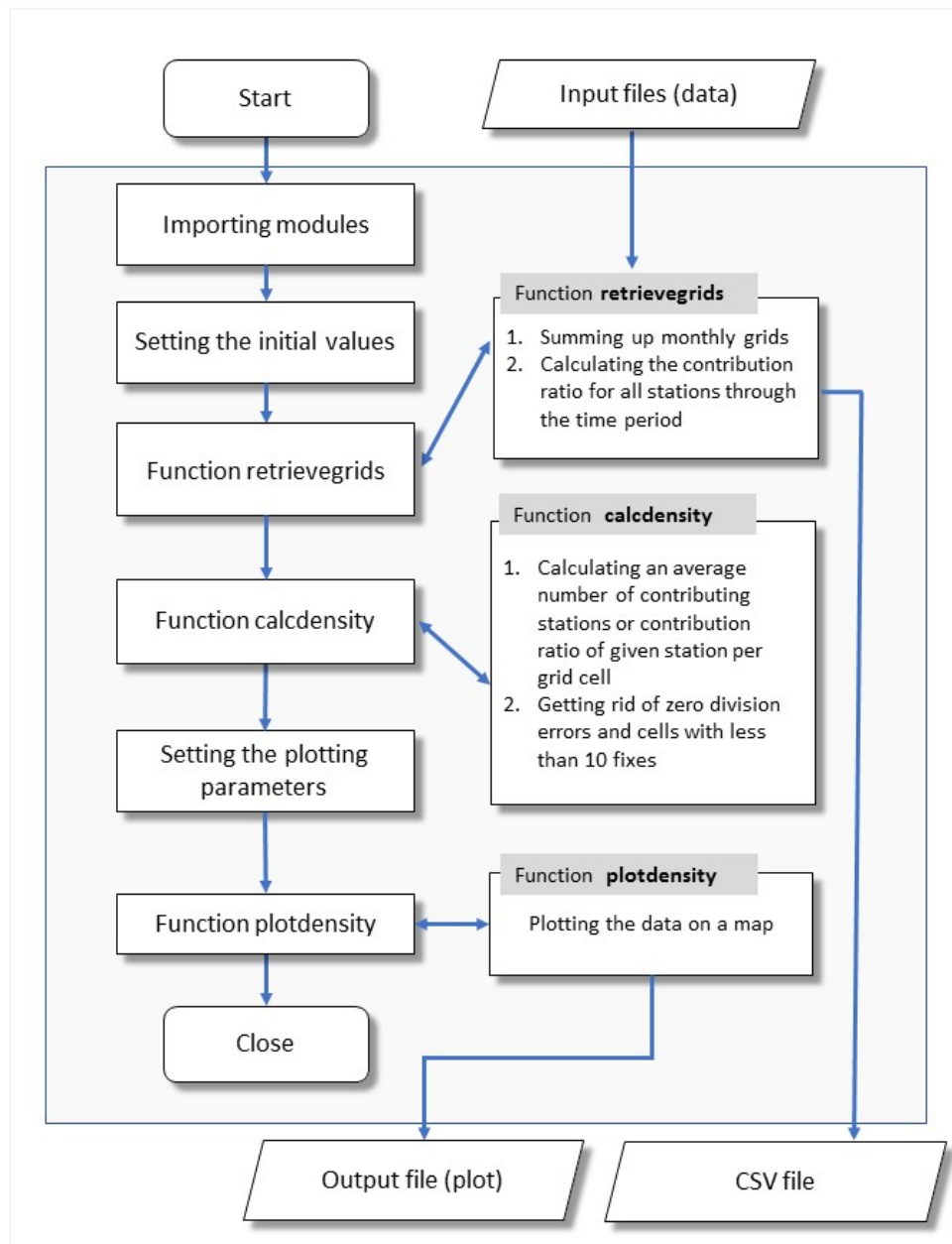
APPENDIXES

Appendix 1. Overall schema of the script for getting a monthly 4D numpy array of total number of fixes per grid cell and total number of contributing stations per grid cell
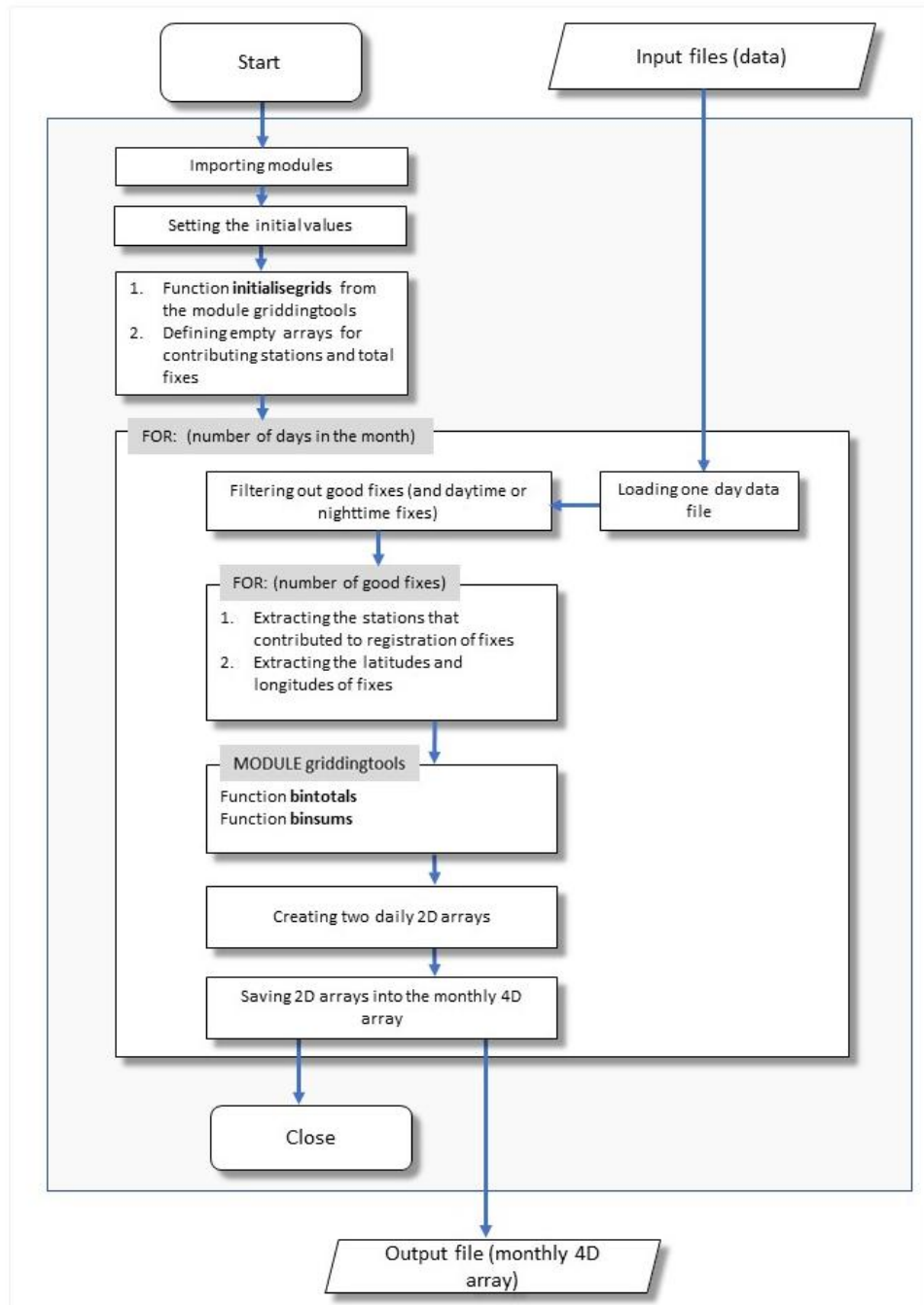
Appendix 2. Overall schema of the script for getting a monthly 4D numpy arrays of total number of fixes and total number fixes detected by a given station per grid cell
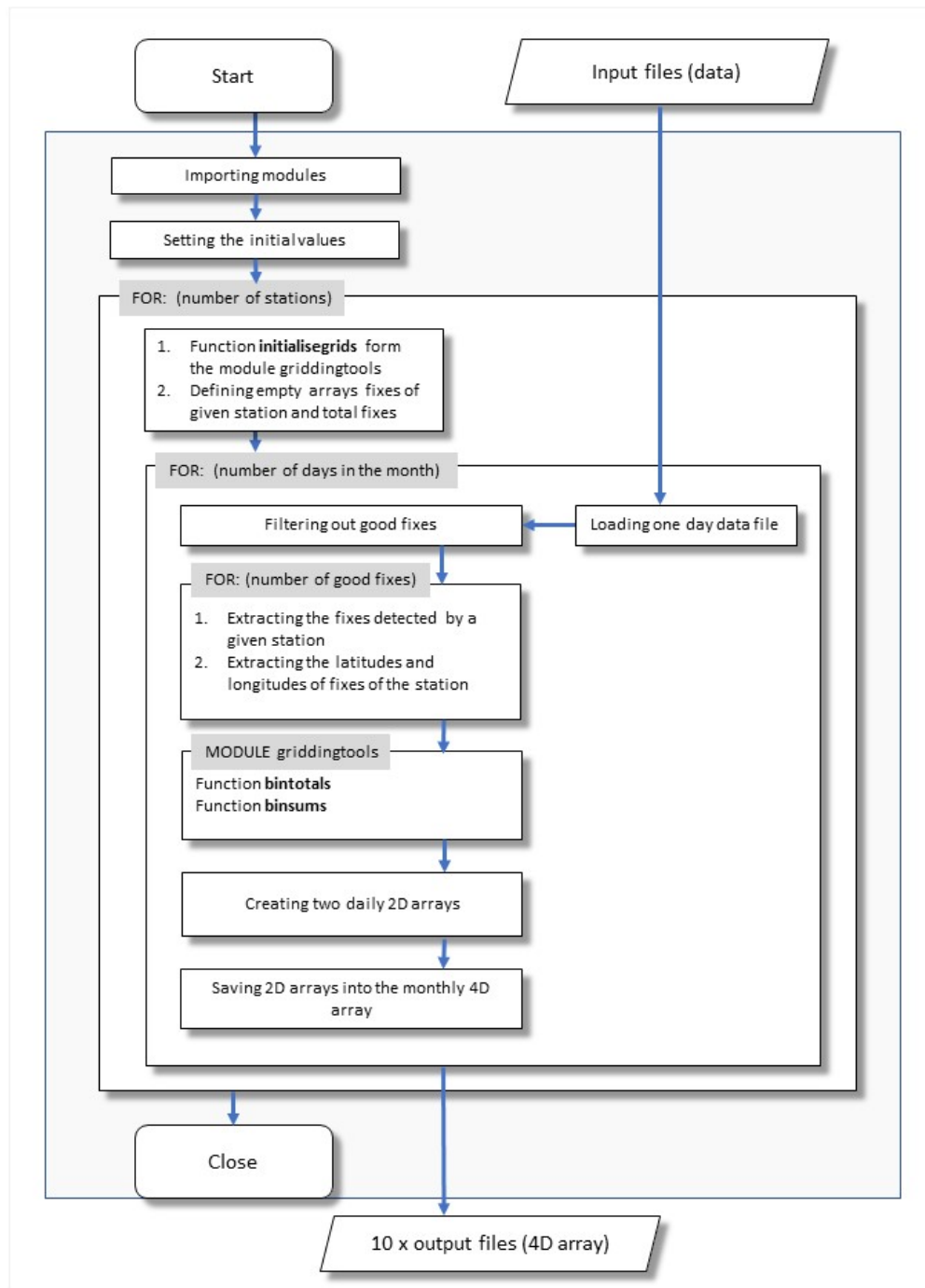
Appendix 3. Overall schema of the script for plotting spatial distribution of contributing stations per fix and spatial distribution of given station contribution ratio per fix

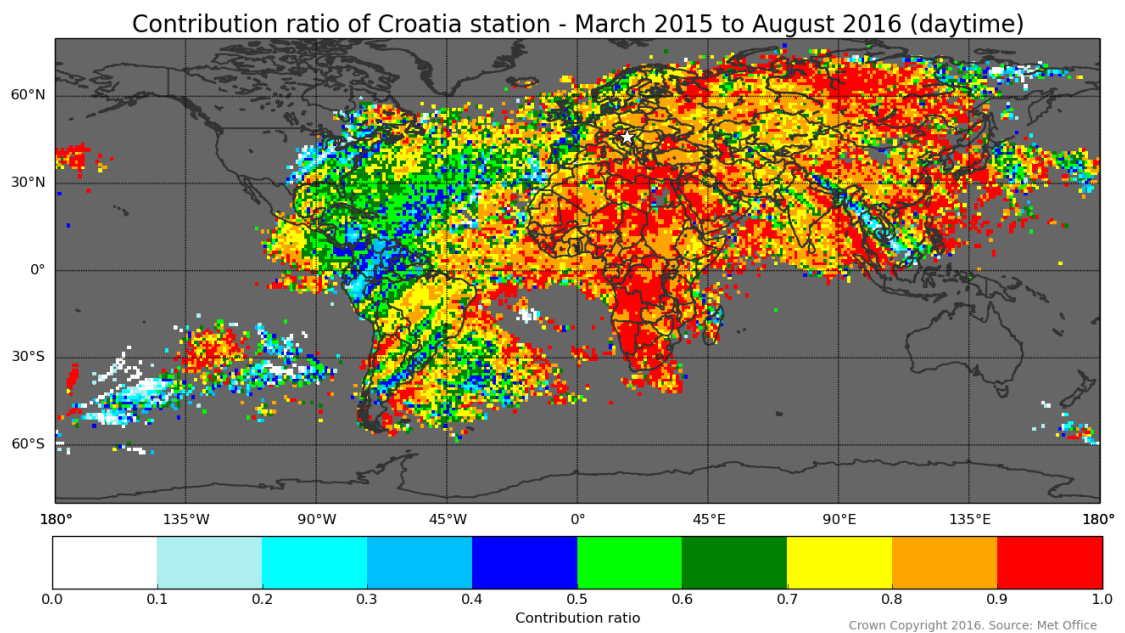**Appendix 4. The average contribution ratio of Payerne station at night and during the day**

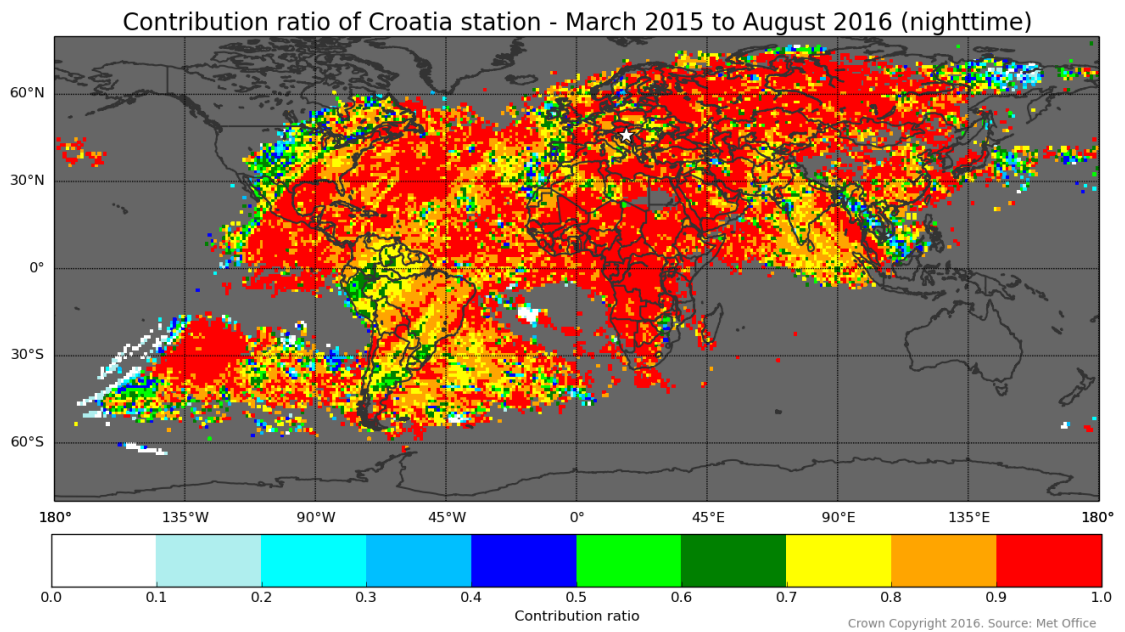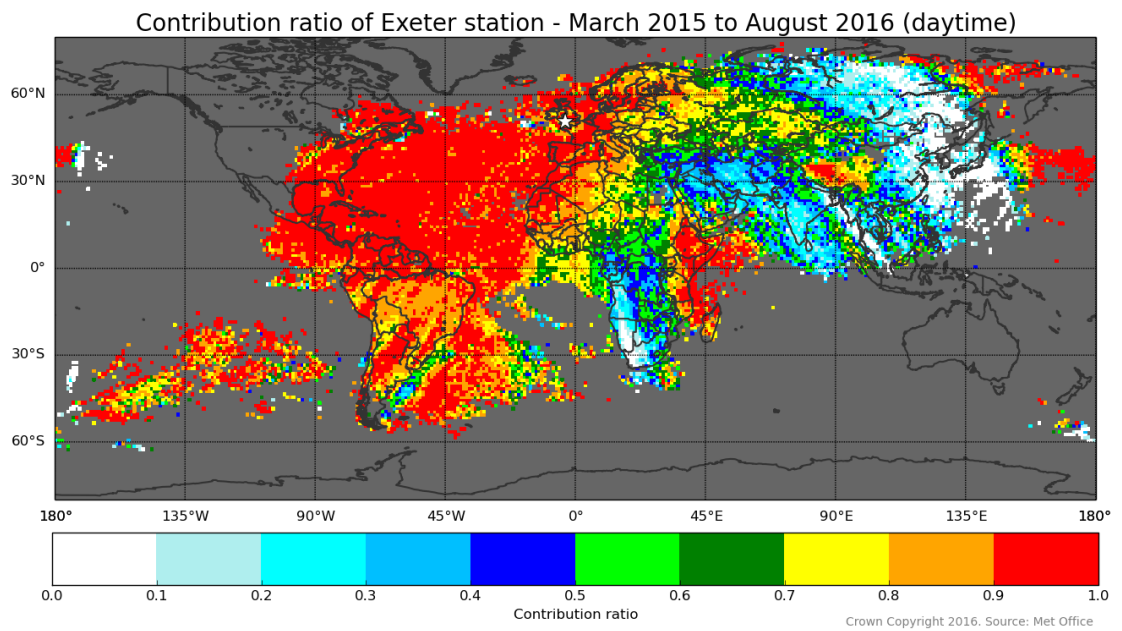Contribution ratio of Payerne station - March 2015 to August 2016 (nighttime)

Contribution ratio of Payerne station - March 2015 to August 2016 (daytime)
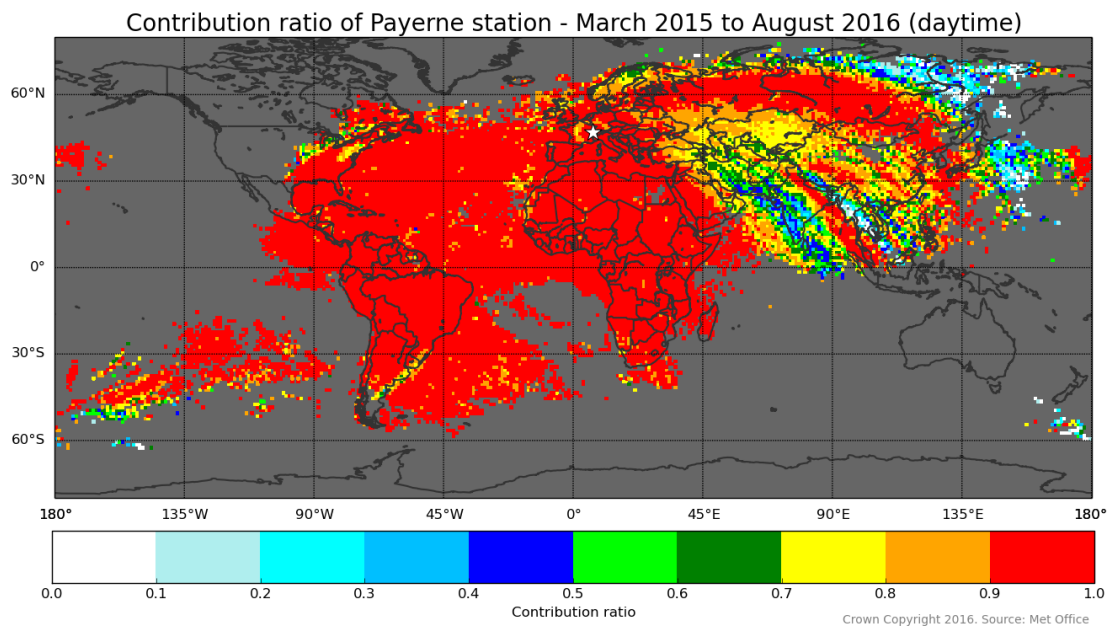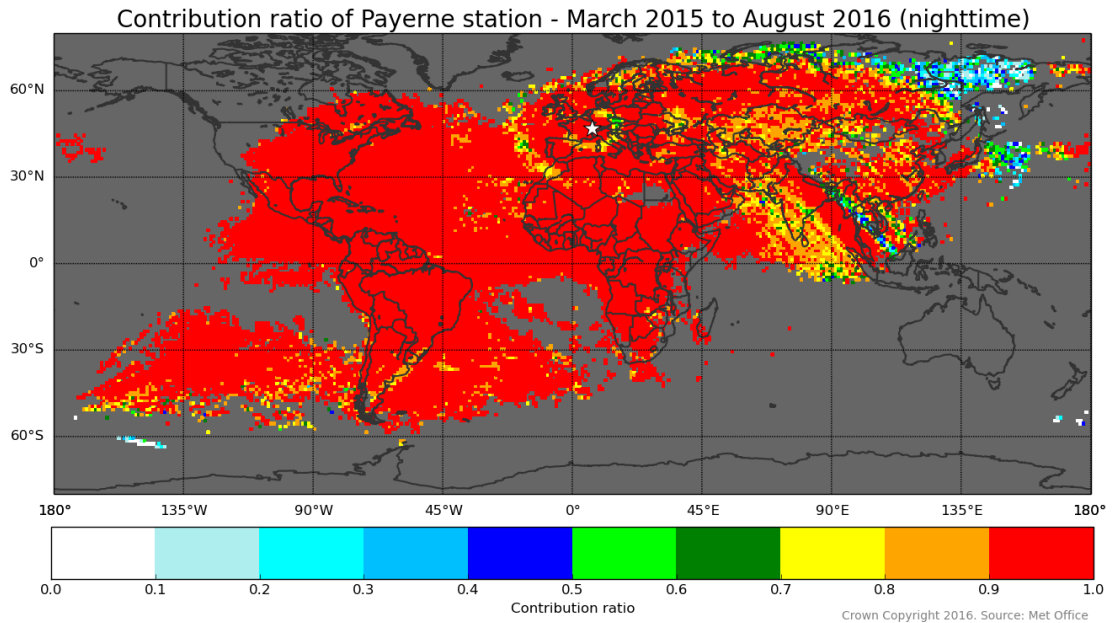
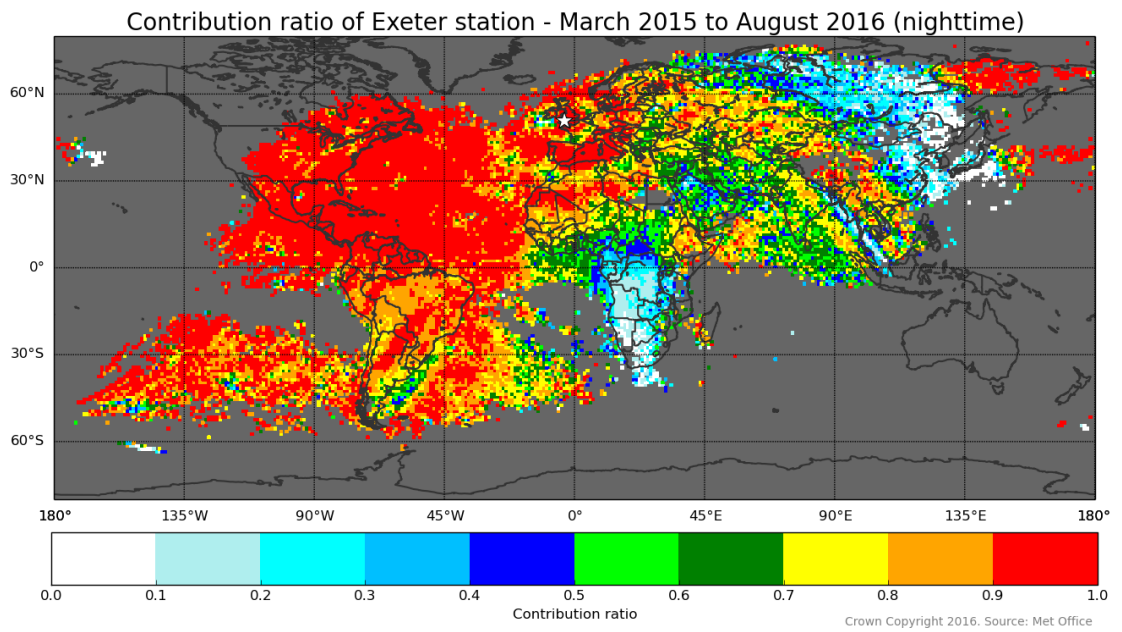**Appendix 5. The average contribution ratio of Eskdale station at night and during the day**

Contribution ratio of Eskdale station - March 2015 to August 2016 (nighttime)

Crown Copyright 2016. Source: Met Office

Contribution ratio of Eskdale station - March 2015 to August 2016 (daytime)

Crown Copyright 2016. Source: Met Office
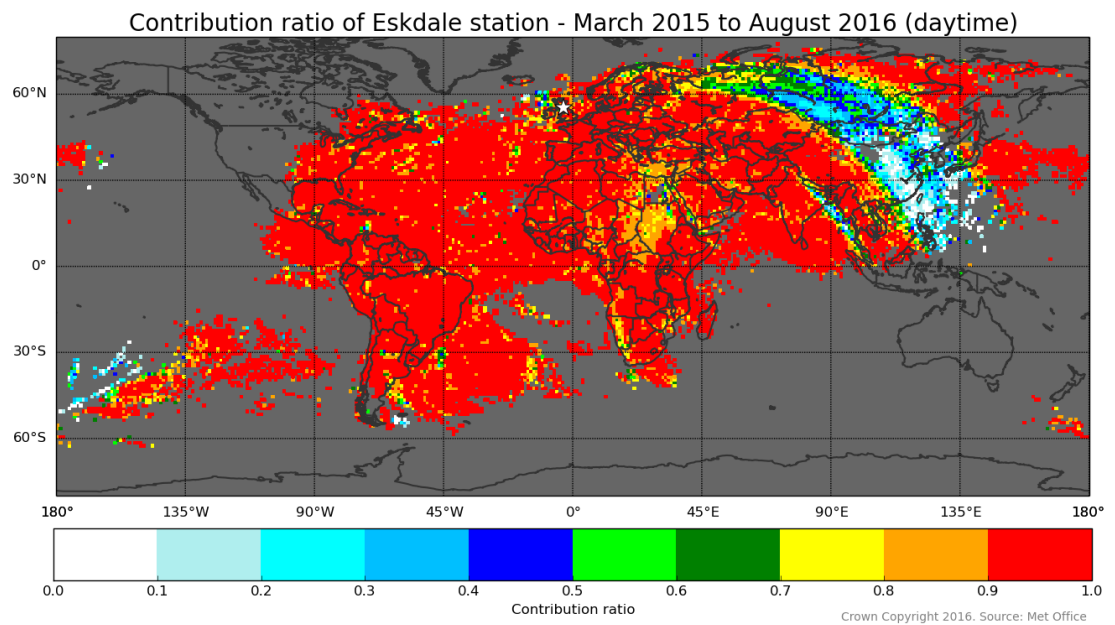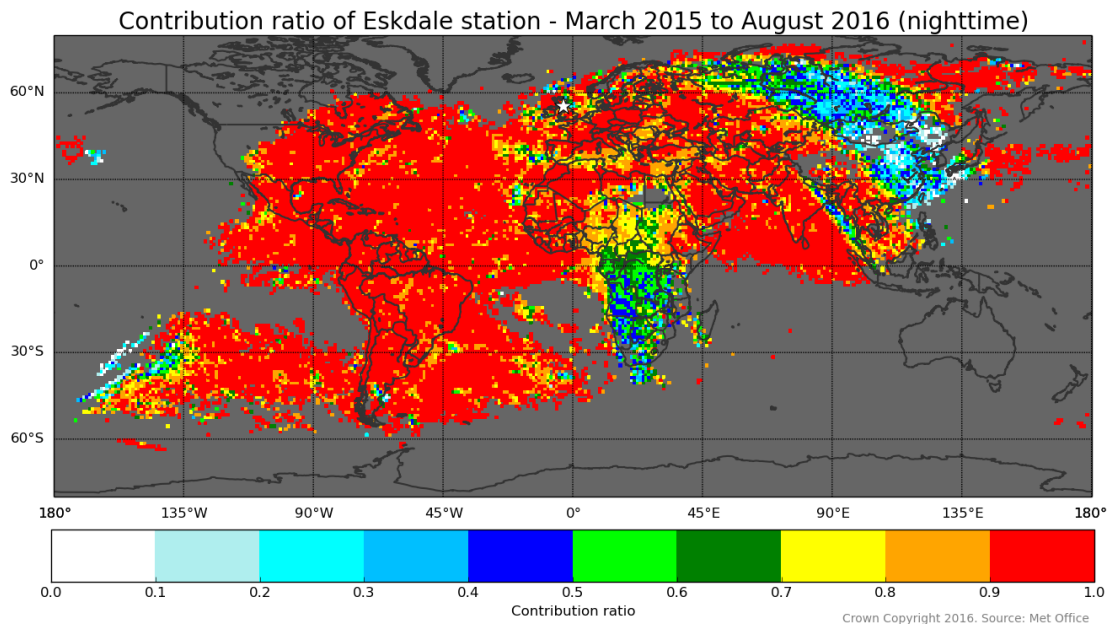
Appendix 6. The average contribution ratio of Norderney station at night and during the day

Contribution ratio of Norderney station - March 2015 to August 2016 (nighttime)

Crown Copyright 2016. Source: Met Office

Contribution ratio of Norderney station - March 2015 to August 2016 (daytime)
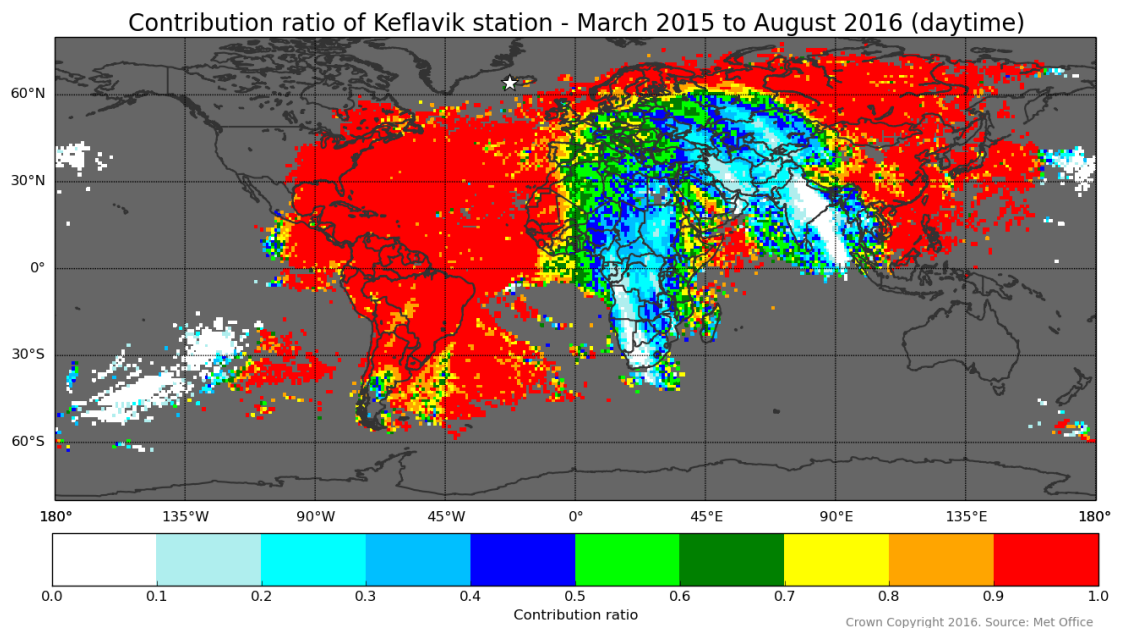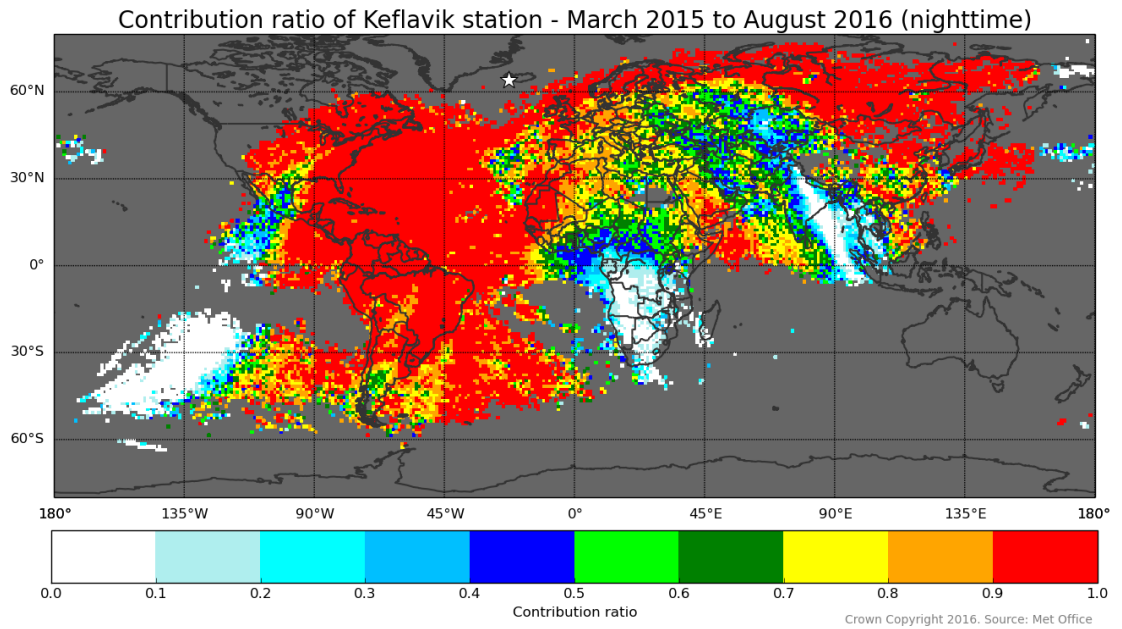

Crown Copyright 2016. Source: Met Office
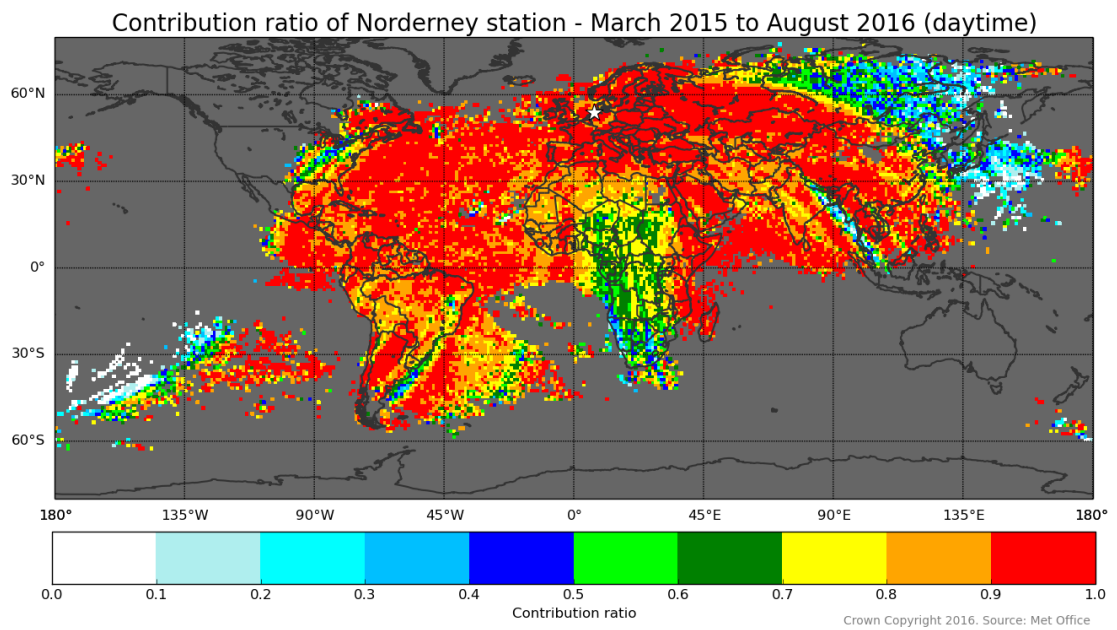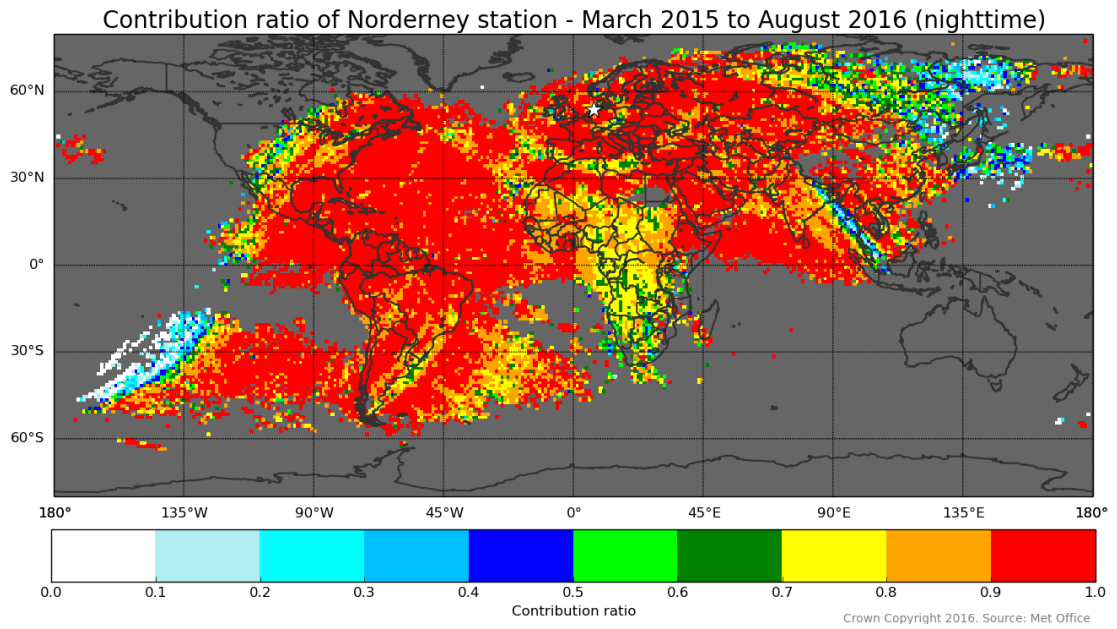
Appendix 7. The average contribution ratio of Croatia station at night and during the day

Contribution ratio of Croatia station - March 2015 to August 2016 (nighttime)

Crown Copyright 2016. Source: Met Office

Contribution ratio of Croatia station - March 2015 to August 2016 (daytime)
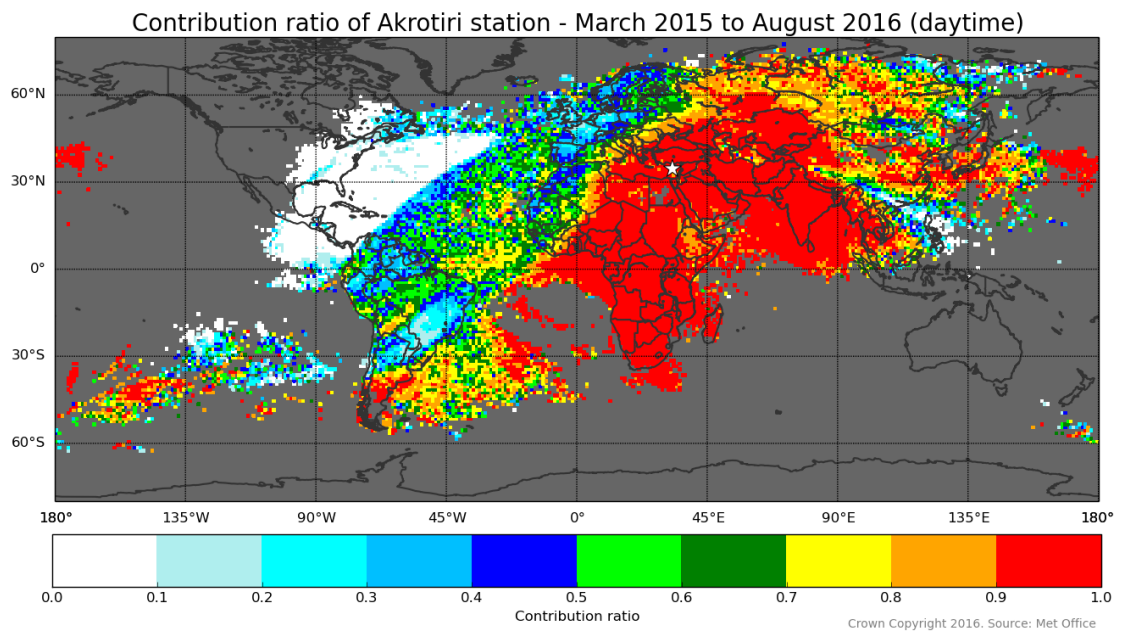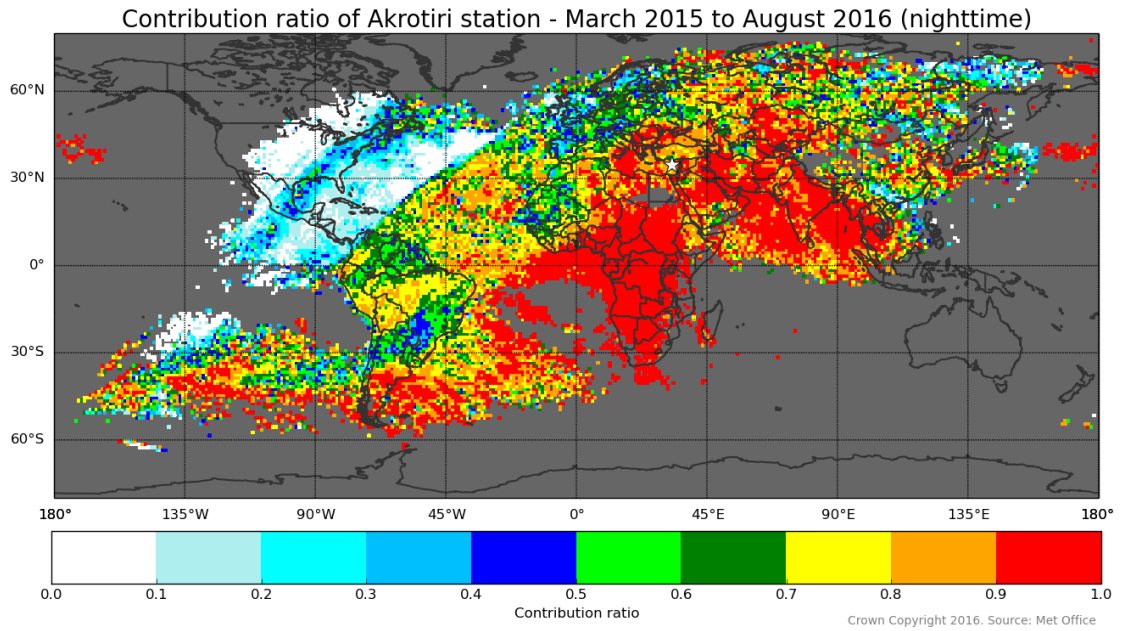
Crown Copyright 2016. Source: Met Office

Appendix 8. The average contribution ratio of Exeter station at night and during the day

Contribution ratio of Exeter station - March 2015 to August 2016 (nighttime)
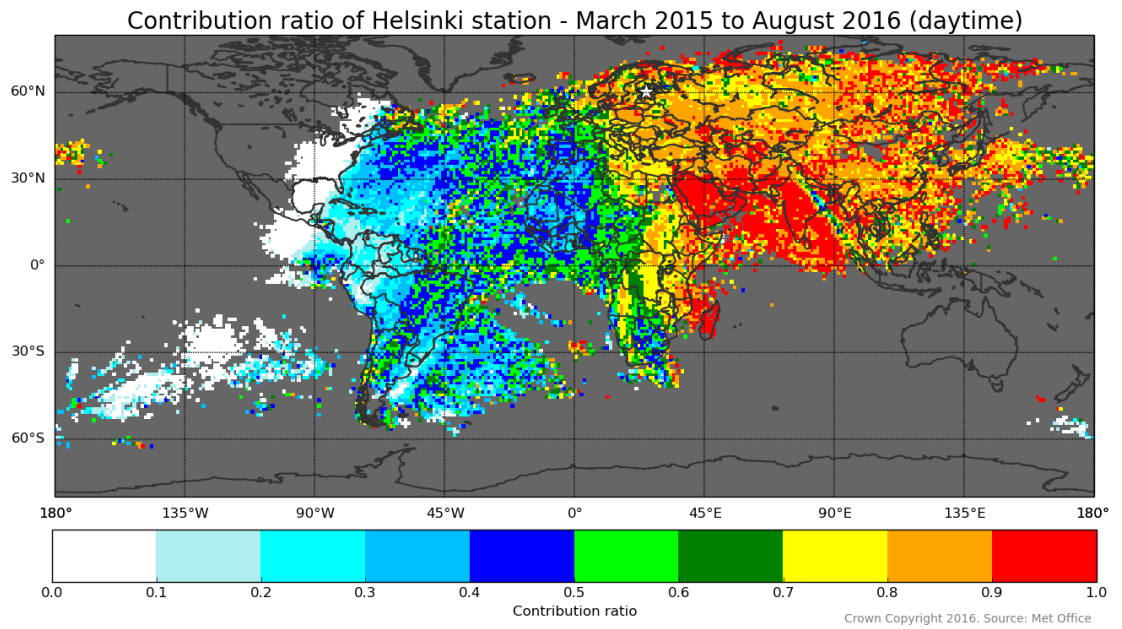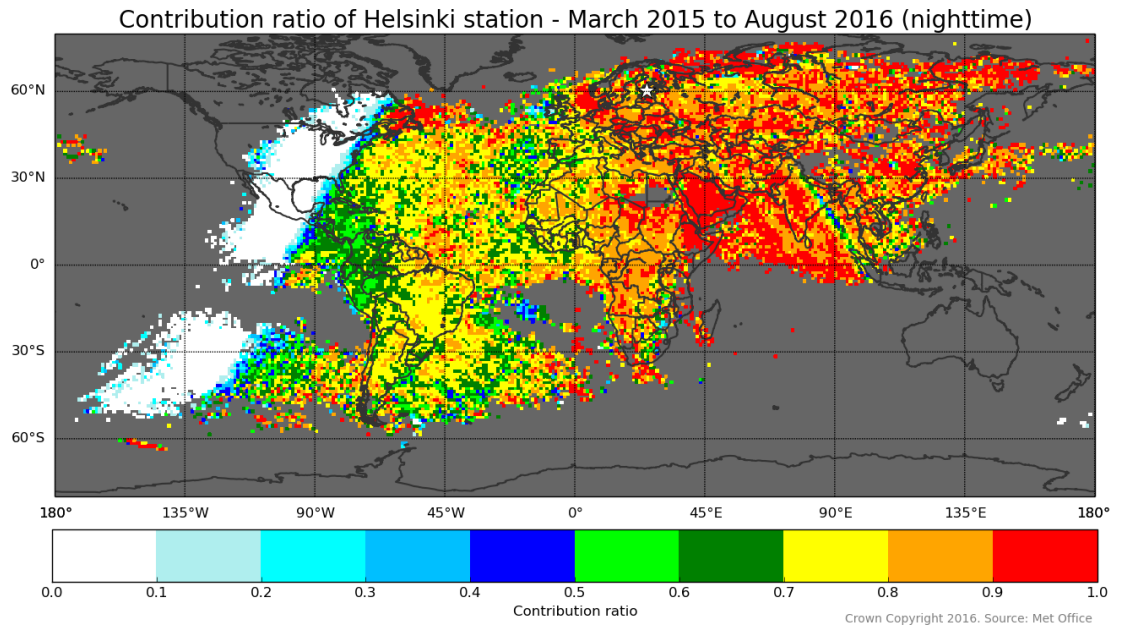

Contribution ratio of Exeter station - March 2015 to August 2016 (daytime)

Appendix 9. The average contribution ratio of Keflavik station at night and during the day

Contribution ratio of Keflavik station - March 2015 to August 2016 (nighttime)

Contribution ratio of Keflavik station - March 2015 to August 2016 (daytime)

Appendix 10. The average contribution ratio of Akrotiri station at night and during the day

Contribution ratio of Akrotiri station - March 2015 to August 2016 (nighttime)

Contribution ratio of Akrotiri station - March 2015 to August 2016 (daytime)

Contribution ratio of Helsinki station - March 2015 to August 2016 (nighttime)

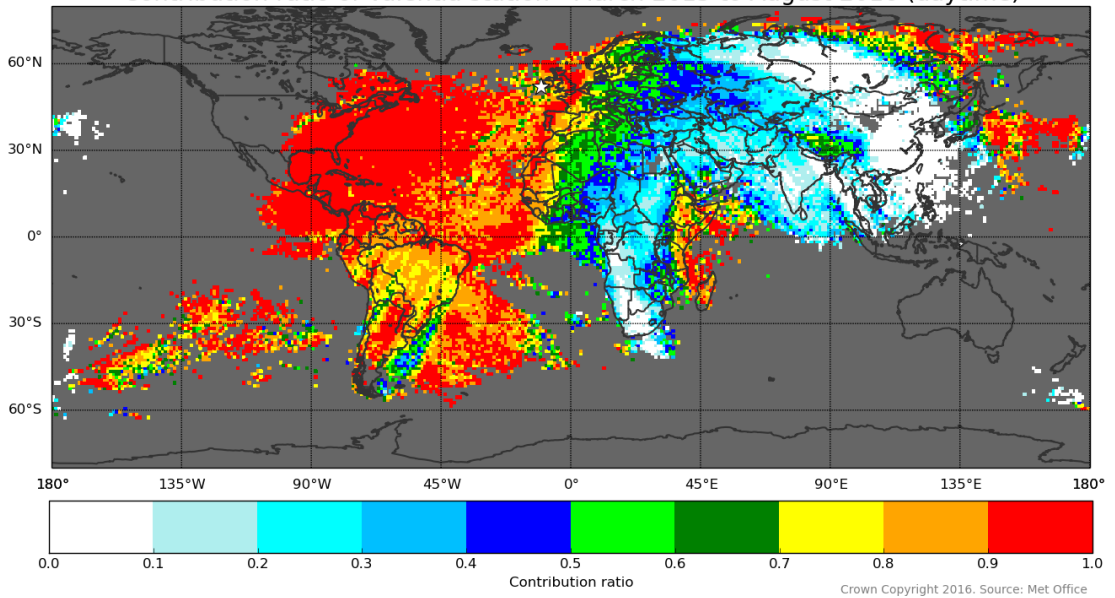Contribution ratio of Helsinki station - March 2015 to August 2016 (daytime)

Appendix 12. The average contribution ratio of Valentia station at night and during the day

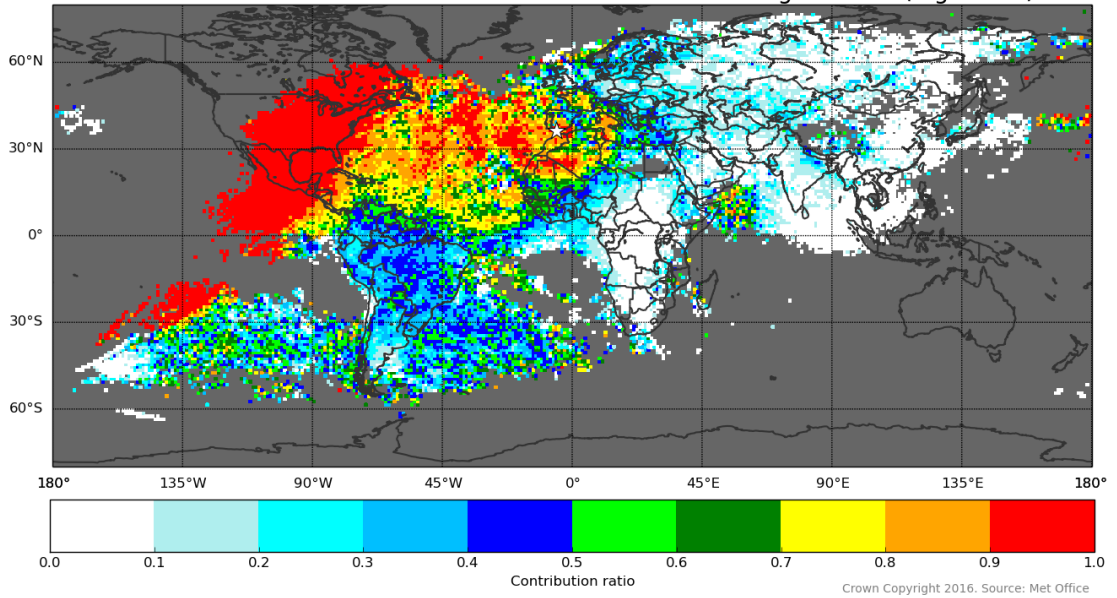Contribution ratio of Valentia station - March 2015 to August 2016 (nighttime)

Crown Copyright 2016. Source: Met Office

Contribution ratio of Valentia station - March 2015 to August 2016 (daytime)
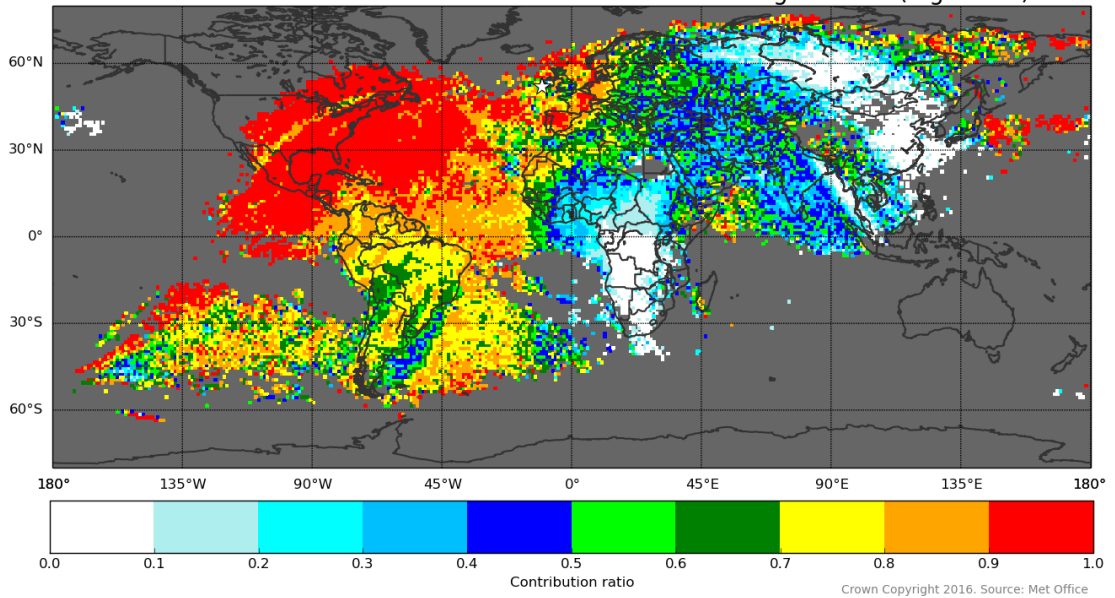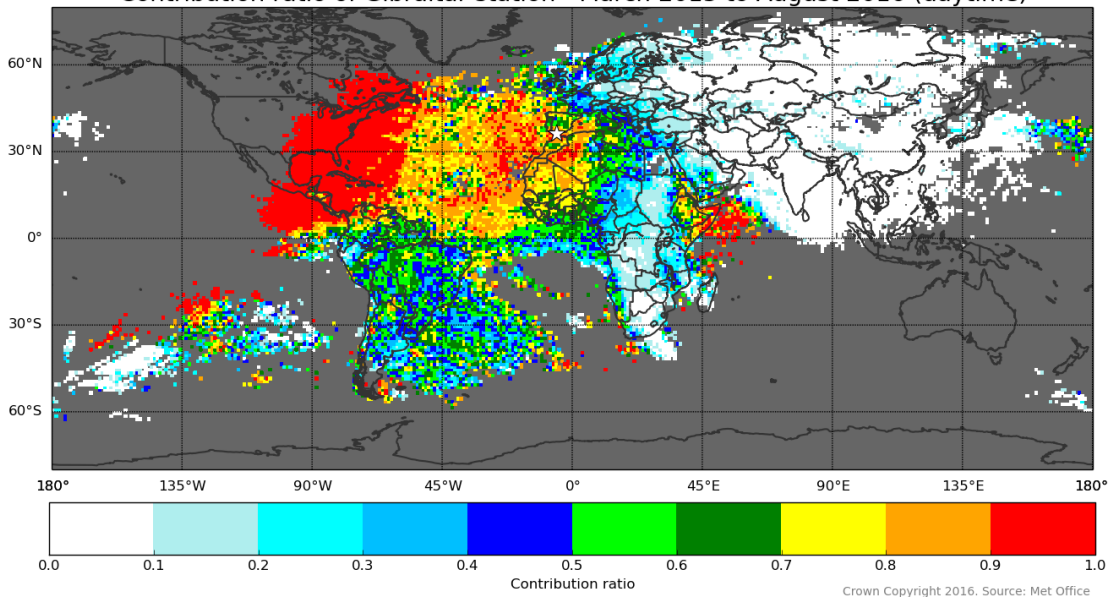
Crown Copyright 2016. Source: Met Office

Appendix 13. The average contribution ratio of Gibraltar station at night and during the day
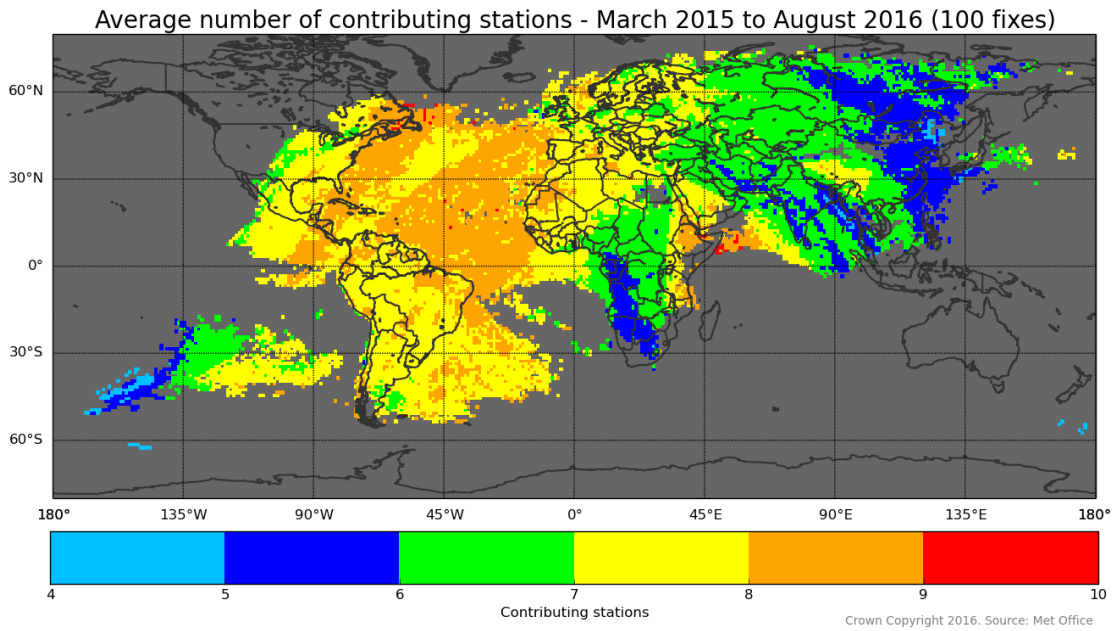
Contribution ratio of Gibraltar station - March 2015 to August 2016 (nighttime)

Contribution ratio of Gibraltar station - March 2015 to August 2016 (daytime)

Appendix 14. The average number of contributing stations for minimum of 100 fixes per grid cell

Average number of contributing stations - March 2015 to August 2016 (100 fixes)

Appendix 15. The average number of contributing stations in winter, spring, summer and autumn for minimum of 100 fixes per grid cell
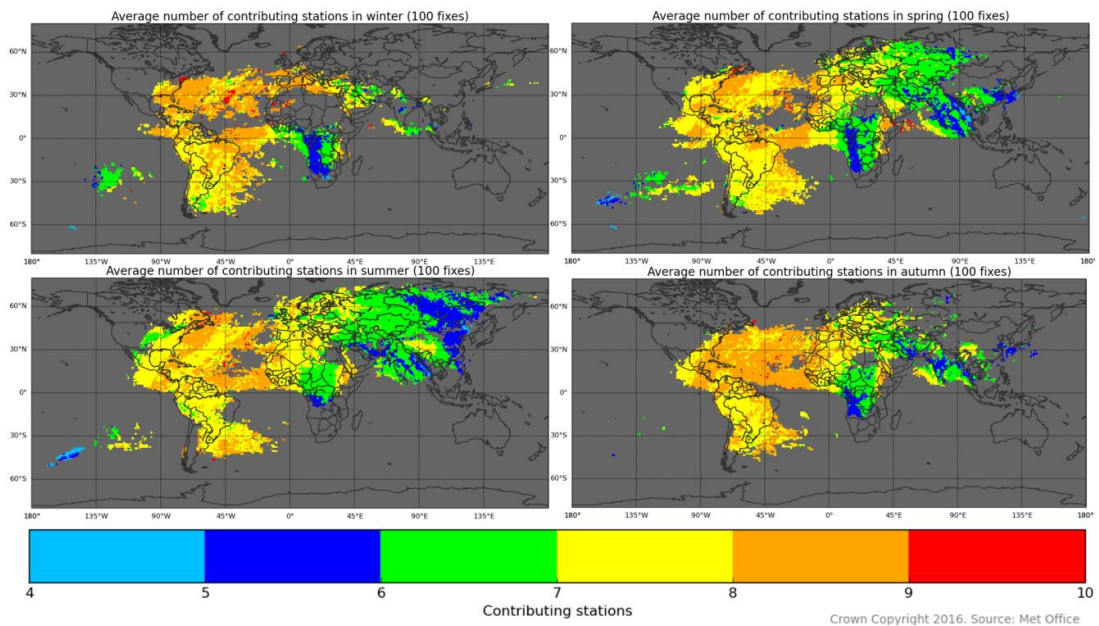
Appendix 16. The average contribution ratio of Akrotiri station with changed color scale in Europe during the day

Contribution ratio of Akrotiri station in Europe - March 2015 to August 2016 (daytime)

Crown Copyright 2016. Source: Met Office
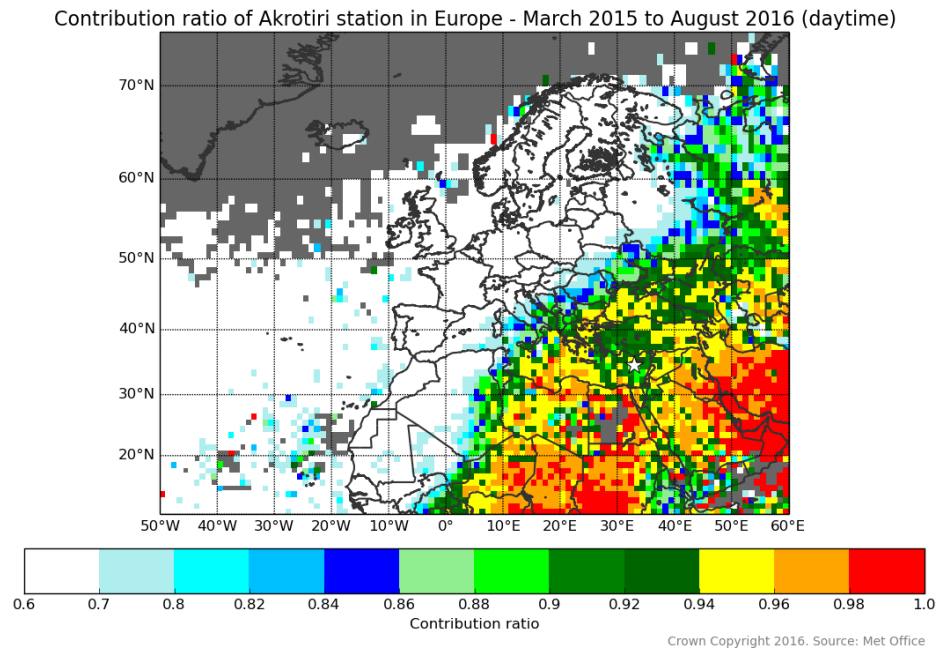
Appendix 17. The average contribution ratio of Helsinki station with changed color scale in Europe at night and during the day

Contribution ratio of Helsinki station in Europe - March 2015 to August 2016

Crown Copyright 2016. Source: Met Office